Astronomy & Astrophysics manuscript no. SN˙Ia˙neut+tp
January 3, 2011

Probing thermonuclear supernova explosions with neutrinos

A. Odrzywolek[1] and T. Plewa[2]

[1] Marian Smoluchowski Institute of Physics, Jagiellonian University, Reymonta 4, 30-059 Cracow, Poland
[2] Department of Scientific Computing, Florida State University, Tallahassee, FL 32306, U.S.A.

Received / Accepted

ABSTRACT

Aims. We present neutrino light curves and energy spectra for two representative Type Ia supernova explosion models: a pure deflagration and a delayed detonation.
Methods. We calculate the neutrino flux from β processes using NSE abundances convoluted with approximate neutrino spectra of the individual nuclei, and the thermal neutrino spectrum (pair+plasma).
Results. Although the two considered thermonuclear supernova explosion scenarios are expected to produce almost identical electromagnetic output, their neutrino signatures appear vastly different allowing for unambiguous identification of the explosion mechanism: a pure deflagration produces a single peak in the neutrino light curve while addition of the second maximum characterizes a delayed-detonation. We identified the following main contributors to the neutrino signal: (1) weak electron neutrino emission from electron captures (in particular on protons, ^{55}Co, and ^{56}Ni) and numerous β-active nuclei produced by the thermonuclear flame and/or detonation front, (2) electron antineutrinos from positron captures on neutrons, and (3) the thermal emission from pair annihilation. We estimate that a pure deflagration supernova explosion at a distance of 1 kpc would trigger about 14 events in the future 50 kt liquid scintillator detector and some 19 events in a 0.5 Mt water Cherenkov-type detector.
Conclusions. While in contrast to core-collapse supernovae neutrinos carry only a very small fraction of the energy produced in the thermonuclear supernova explosion, the SN Ia neutrino signal provides information that allows to unambiguously distinguish between different possible explosion scenarios. Such studies will become feasible with the next generation of proposed neutrino observatories.

Key words. hydrodynamics – neutrinos – nuclear reactions, nucleosynthesis, abundances – stars: supernovae: general

1. Introduction

The origins of Type Ia supernovae (SN Ia) remain one of the major unsolved problems of stellar evolution (Höflich & Stein 2002; Kuhlen et al. 2006; Piro 2008; Zingale et al. 2009). The commonly accepted theoretical framework considers an explosion scenario in which a massive white dwarf slowly gains mass in the process of accretion from a non-degenerate companion (Whelan & Iben 1973; Yoon & Langer 2003; Han & Podsiadlowski 2004; Meng & Yang 2010). Alternatively, the degenerate matter might be ignited in the process of a violent merger of binary white dwarfs (Iben & Tutukov 1984; Webbink 1984; Han 1998). The latter channel might be a dominant source of thermonuclear events in early type galaxies (Gilfanov & Bogdán 2010; Wang et al. 2010), while there is no consensus as to which evolutionary process dominates in other environments (Scannapieco & Bildsten 2005; Raskin et al. 2009; Ruiter et al. 2009; Schawinski 2009).

Our progress toward understanding these events is hampered by relatively low luminosity of their progenitors, and to date the evidence is largely circumstantial and exclusively indirect (Ruiz-Lapuente et al. 2004; Badenes et al. 2007; Schawinski 2009; Gilfanov & Bogdán 2010). This stays in contrast with numerous identifications of core-collapse progenitors (Smartt 2009; Leonard 2009, and references therein). Furthermore, the nature of the explosion process is very uncertain though it is commonly accepted that the energy source of the explosion is a thermonuclear burn (Hoyle & Fowler 1960). In case of a single degenerate channel, the nuclear fuel is expected to burn first subsonically (Nomoto et al. 1976) with a likely transition to detonation at a later time (Khokhlov 1991; Woosley & Weaver 1994). It is much less clear what the ultimate fate of the merger is (Hachisu et al. 1986; Saio & Nomoto 1985; Yoon et al. 2007; Pakmor et al. 2010), and perhaps additional routes to explosion are admissible (Podsiadlowski et al. 2008; Podsiadlowski 2010, and references therein). These issues along with the role that SN Ia play in studies of the early universe (Sandage & Tammann 1993; Riess et al. 1998; Phillips 2005; Wood-Vasey et al. 2007; Ellis et al. 2008; Riess et al. 2009; Kessler et al. 2009) motivate search for additional sources of information about thermonuclear supernovae, and in particular about the explosion process.

Neutrinos are a proven source of the unique information about astrophysical objects and phenomena, the Earth (Smirnov 2009; Araki et al. 2005; Dye 2006), but also engineering systems such as nuclear power plants (Bowden 2008; Lhuillier 2009; Learned 2005; Guillian 2006). The Sun is one of the best-studied astrophysical neutrino sources thanks to its proximity and constancy of the ν_e flux (Bahcall 1989). Solar neutrino studies were first conducted using radiochemical detectors (Cleveland et al. 1998; Hampel et al. 1999) and more recently also in real-time (BOREXINO Collaboration et al. 2008; Arpesella et al. 2008; Fukuda et al. 2001; Ahmad et al. 2001). For contemporary non-solar neutrino experiments, the solar neutrino signal due to the dominant reactions (pp, ^{8}B) constitutes rather undesirable background. However, supernova SN 1987A (Arnett et al. 1989) has been clearly observed in neutrinos in many detectors (Van Der Velde et al. 1988; Hirata et al. 1987; Galeotti et al. 1987; Alekseev et al. 1987) despite its nearly extragalactic distance

Send offprint requests to: A. Odrzywolek e-mail: andrzej.odrzywolek@uj.edu.pl

(∼50 kpc). The event has been the main trigger for intensive theoretical studies and modeling in the recent years (Immler et al. 2007; Nakahata, M. and Sobel, H. 2007) while a possibility of neutrino detection and obtaining neutrino energy spectra from core-collapse supernovae (Burrows 1990; Keil et al. 2003) attracted constant attention of theorists (Kistler et al. 2008; Fogli et al. 2005a; Ando et al. 2005; Fogli et al. 2005b) and stimulated experimental developments (Suzuki 2001; Learned 2004). Neutrino detection is a mature field of research nowadays. Noteworthy, a stellar core-collapse at a distance < 4 kpc will produce a signal large enough to saturate the Super-Kamiokande detector (Nakahata 2007). Therefore it is natural to consider detectability of neutrinos from previously ignored sources, including thermonuclear supernova events.

As originally suggested by Nomoto et al. (1993), the neutrino signal produced by the thermonuclear deflagrations offers direct insight into the explosion process. Clearly, such observations would be extremely helpful in directing future SN Ia research possibly allowing for distinguishing between various stellar evolution and explosion scenarios. A striking differences between neutrino emission from deflagrations and delayed detonations has been noted by Nomoto et al. (1993). More recently, in a series of articles Kunugise & Iwamoto (Iwamoto & Kunugise 2006; Kunugise & Iwamoto 2007) studied the ν_e light curve and spectra from the standard W7 explosion model (Nomoto et al. 1984) and discussed detectability of such event by the Super-Kamiokande detector. We aim to extend those early studies to recent multi-dimensional thermonuclear supernova explosion models. We obtain supernova neutrino light curves and energy spectra for pure deflagration and delayed detonation explosion models. We show that the predicted neutrino signatures are markedly different in those two cases and can be used to identify the explosion mechanism.

2. Neutrino emission from thermonuclear supernovae

Neutrino emission from a Type Ia supernova is considered negligible in most of the thermonuclear explosion models because weak interaction rates are too slow compared to the hydrodynamic timescale (see Arnett 1996, Sect. 9.1) and the matter is essentially completely transparent to neutrinos. However, it is conceivable that if the amount of the energy emitted *via* neutrinos is significant compared to the energy produced in the thermonuclear burning, the neutrino cooling may play an important role in the explosion dynamics. In either case, neutrinos may provide important insights into the SN Ia explosion mechanism.

Neutrino emission from the existing SN Ia explosion models can be computed by post-processing snapshots of the hydrodynamical simulations. For the thermal neutrino emission this is a straightforward procedure as the neutrino spectrum depends only on the temperature and the (electron) density of the plasma. For weak nuclear processes, we have to know the isotopic composition of the plasma. Given the current computational resources, it is unfeasible to include large nuclear reaction networks in multidimensional explosion model. The situation, however, is not completely hopeless as the hottest regions associated with thermonuclear flames and detonations, and where the neutrino emission is expected to be relatively high, are in the nuclear statistical equilibrium (NSE) (see Clayton 1984, Sect. 7.2). Under the NSE conditions, isotopic abundances are determined solely by the thermodynamic properties of the plasma. Therefore, in the most important regions of the exploding star, we are again able to post-process models and compute required abundances. Once isotopic composition is known, computing a neutrino emission is relatively straightforward (Kunugise & Iwamoto 2007).

In NSE, the isotopic composition of the matter is fully determined by the density, temperature, and electron density of the plasma (Clifford & Tayler 1965a,b). The NSE conditions are characterized by

1. very high temperature to break-up the most strongly bound nuclei;
2. evolutionary timescale long enough to allow for rearranging of nucleons into equilibrium nuclei *via* strong/electromagnetic interactions.

Such conditions can be found in the iron cores of pre-supernova stars, during core-collapse, and last but not least, during thermonuclear burn in Type Ia supernovae. More recently, protoneutron star evolution and accretion induced collapse recently has been analyzed from this point of view by Arcones et al. (2010).

For completeness we will shortly discuss major properties of the considered neutrino emission processes. Model neutrino spectra are computed with help of the PSNS code (Odrzywolek 2005-2010).

2.1. Sources of neutrinos

2.1.1. Thermal processes

Three "classic" neutrino processes,

$$e^- + e^+ \to \nu_{e,\mu,\tau} + \bar{\nu}_{e,\mu,\tau} \tag{1a}$$

$$\gamma^*_{L,T} \to \nu_{e,\mu,\tau} + \bar{\nu}_{e,\mu,\tau} \tag{1b}$$

$$\gamma + e^- \to e^- + \nu_{e,\mu,\tau} + \bar{\nu}_{e,\mu,\tau} \tag{1c}$$

are the major source of the so-called thermal neutrinos (Munakata et al. 1985; Schinder et al. 1987; Esposito et al. 2003): annihilation of the e^+e^- pairs into neutrinos (Eq. (1a), Misiaszek et al. 2006); plasmon decay, (Eq. (1b), Braaten 1991; Braaten & Segel 1993), and photoemission (Eq. (1c), Dutta et al. 2004). Emissivity and spectra of these neutrinos are uniquely determined by the plasma temperature and electron density. All flavors of the neutrinos are produced in these processes: $\nu_e, \bar{\nu}_e, \nu_\mu, \bar{\nu}_\mu, \nu_\tau, \bar{\nu}_\tau$. Following the standard theory of electroweak interactions, fluxes for all flavors are quite similar, however some differences exist between the electron and μ/τ flavors. Additionally, because of the parity violation, neutrino and antineutrino energies are not equal under degenerate conditions considered here (Odrzywołek 2007; Misiaszek et al. 2006).

Pair annihilation neutrino fluxes and spectra were calculated according to Misiaszek et al. (2006). This approach is superior to both Itoh et al. (1996a) method typically used in stellar evolution calculations (because the neutrino flavors are not summed up) and Bruenn (1985); Burrows & Thompson (2002) method used for core-collapse supernova modeling (because the electron rest mass is not neglected).

Plasma neutrino flux and spectrum has been calculated according to Odrzywołek (2007). Procedures were tested against Itoh et al. (1992), Kohyama et al. (1994), and Itoh et al. (1996b) tables (calculated using a slightly different dispersion relations for plasmons) with reasonable agreement, and also against recent calculations of Kantor & Gusakov (2007). In the latter case, the results are equal up to the machine precision.

Photoneutrino process, as well as thermal processes of a lesser importance (e.g. neutrino bremsstrahlung, cf. Yakovlev

et al. 2001) were omitted in our calculations, due to lack of relevant results on the neutrino spectrum. This may lead to negligible underestimate of the thermal neutrino flux.

2.1.2. Weak nuclear processes

Weak processes, namely electron/positron captures on both nucleons and nuclei and $\beta^{\pm}$ decays are extremely important in the astrophysical environments. They are essential ingredients of e.g. massive star evolution (especially pre-supernova phase, Kutschera et al. 2009), core-collapse supernovae and thermonuclear explosions: x-ray flashes, novae and SN Ia. Weak nuclear neutrino processes usually work in the cycles like:

$$\begin{array}{ccc} e^- + (A,Z) & \longrightarrow & (A,Z-1) + \nu_e \\ \uparrow & & \downarrow \\ \bar{\nu}_e + e^- + (A,Z) & \longleftarrow & (A,Z-1) \end{array} \tag{2a}$$

$$\begin{array}{ccc} e^+ + (A,Z-1) & \longrightarrow & (A,Z) + \bar{\nu}_e \\ \uparrow & & \downarrow \\ \nu_e + e^+ + (A,Z-1) & \longleftarrow & (A,Z) \end{array} \tag{2b}$$

and the total number of emitted neutrinos per nucleus is usually not equal to 1, in contrast to terrestrial beta decays and electron captures.

One of the most important motivations for inclusion of weak nuclear rates was a search for nuclei producing $\bar{\nu}_{\rm e}$ or $\nu_{\rm e}$ leading to very strong signal in the detectors (in analogy to Solar ^{8}B neutrinos). Such a nuclei must meet three conditions: (1) have to be abundant in NSE, (2) posses very high β or capture rate, and (3) emit energetic $\nu_{\rm e}$ or $\bar{\nu}_{\rm e}$ with energies above, say, 10-15 MeV. Unfortunately, inspection of the Figs. 6,7 and Table 2 reveals no such nuclei present in our study. Strong degeneracy during initial stage of the deflagration enhances transitions with relatively high energy neutrinos (we thank G. Fuller for pointing this important aspect to us). For some nuclides, e.g. ^{57}Zn, ^{54}Cr and ^{28}P, average neutrino energy $\langle \mathcal{E}_{\nu_e} \rangle$ reach 15 MeV. NSE abundance and therefore neutrino flux from these nuclides is negligible (cf. Fig. 6). The nucleus producing the highest elastic scattering event rate is ^{55}Co, but equally important are electron captures on protons. The case of ^{54}Co, with quite high average neutrino energy (≈9 MeV) is very interesting and deserving more detailed analysis.

Some of the nuclei produce also relatively energetic antineutrinos, e.g. $\langle \mathcal{E}_{\nu_e} \rangle \approx 6$ MeV for ^{56}V and ^{58}V during both deflagration and detonation stages. The corresponding flux however is small compared to thermal (pair) and $e^+(n,p)\bar{\nu}_e$ electron antineutrinos fluxes. We conclude that β processes involving nuclei provide only a negligible contribution to the $\bar{\nu}_e$ flux.

While the energy loss rate as well as decrease of the electron fraction due to weak processes were extensively studied in the past (Fuller et al. 1980, 1982a,b; Oda et al. 1994; Aufderheide et al. 1994a,b; Caurier et al. 1999; Langanke & Martínez-Pinedo 2000; Nabi & Klapdor-Kleingrothaus 1999; Seitenzahl et al. 2009; Juodagalvis et al. 2009, and references therein), relatively little is known about the combined energy spectrum of these neutrinos (Langanke et al. 2001; Odrzywolek 2009). Typically, the spectrum is integrated in advance and the results are tabulated. This approach saves both computer memory and computing time. To restore information about the spectrum, a simple parametrization (e.g. the Fermi-Dirac distribution) is assumed (see, e.g. Pons et al. 2001). We employ a similar method here. However, some fine details of the nuclear structure reflected in the neutrino spectrum are lost when using this approach. In certain conditions, this may lead to a serious underestimate of the neutrino signal, especially in the high energy ($\mathcal{E}_\nu > 10$ MeV) tail. With this in mind, our results provide a lower detection threshold for the neutrino signal. Furthermore, some newest results suggest an upward revision of the crucial ^{55}Co electron capture rate by up to two orders of magnitude (Nabi & Sajjad 2008). Such findings seem however staying in conflict with nucleosynthesis results, in particular with the observed degree of neutronization of the ejecta (Nomoto et al. 1997; Isern et al. 1993; Thielemann 1984; Iwamoto et al. 1999).

Our calculations of the weak nuclear neutrino emission proceed as follows. In contrast to the thermal neutrino emission, the contribution due to weak nuclear processes to the neutrino signal cannot be calculated solely based on the thermodynamic properties of matter. Such calculations in general require detailed knowledge of the isotopic composition. Typically, the composition is a result of the long and complicated history of the astrophysical object. As the electron fraction has not been calculated consistently in the adopted explosion models, we assume $Y_{\rm e} = 0.5$. This value corresponds to the initial electron fraction of the progenitor with 50/50 carbon/oxygen composition mix used in the explosion calculations[1]. In more realistic models, the electron neutrino emission would result in decreasing $Y_{\rm e}$. For example, the NSE abundance of ^{55}Co nucleus, which significantly contributes to the $\nu_{\rm e}$ flux, decreases rapidly for $Y_{\rm e} < 0.5$.

The remaining required information about the matter density, ρ, and temperature, T, is obtained from the actual explosion model. We consider only regions where the NSE state can be established on a timescale shorter than the explosion timescale. The NSE timescale can be approximated as (Khokhlov 1989, 1991)

$$\tau_{\rm NSE} \sim \rho^{0.2} e^{179.7/T_9 - 40.5} \text{ s}. \tag{3}$$

For the reference NSE threshold temperature, $T_{\rm NSE} = 5 \times 10^9$ K ($T_9 = 5$, kT≈0.432 MeV) , adopted after Kunugise & Iwamoto (2007) and the characteristic density of $\rho = 10^9$g cm^{-3}, the NSE timescale is, $\tau_{\rm NSE} \approx 0.66$ s, and is shorter than than the explosion timescale, $\tau_{\rm exp} \approx 1$ s.

To estimate sensitivity of the results to the assumed NSE threshold temperature, we performed several additional calculations with the threshold temperature $T_9 = 6$ (kT≈0.517 MeV, $\tau_{\rm NSE} \sim 10^{-3}$ s). This resulted in the total neutrino flux reduced by a few percent. The remaining non-NSE zones were omitted from weak neutrino emission calculations.[2] Their contribution remains unknown at present, but it is unlikely to be important.

For zones with $T > T_{\rm NSE}$, the NSE abundances were calculated using an 800 isotope network up to ^{97}Br (Odrzywolek 2009). From the NSE abundances, we selected nuclei (188 nuclides) for which weak rates have been tabulated by Fuller et al. (1980, 1982a,b). Model energy spectra for neutrinos from electron captures on protons and for antineutrinos from positron captures on neutrons and neutron decay were calculated using

$$\frac{dR_\nu}{d\mathcal{E}_\nu} = \left(\frac{\ln 2}{m_e^5}\right) r_{eff} \Theta\left(\pm\mathcal{E}_\nu \mp Q_{eff} - m_e\right) \frac{\mathcal{E}_\nu^2 (\pm\mathcal{E}_\nu \mp Q_{eff}) \sqrt{(\mathcal{E}_\nu - Q_{eff})^2 - m_e^2}}{1 + e^{(\mathcal{E}_\nu - Q_{eff} \mp \mu)/kT}}, \tag{4}$$

where R_ν is the particle production rate per unit volume and time, $\mathcal{E}_\nu$ is the neutrino energy, r_{eff} and Q_{eff} describe adopted

[1] In more realistic progenitor models, $Y_{\rm e}$ should be slightly below 0.5 due to core burning prior to the explosion (Piro & Bildsten 2008) and/or variation in the initial chemical composition of the progenitor star on the main sequence (Timmes et al. 2003).

[2] Those regions produce neutrinos from decaying beta-unstable nuclides, e.g. ^{56}Ni. This process does not depend on temperature.

parametrization (see Langanke et al. 2001, for details), Θ is the unit step function, upper and lower sign correspond to captures and decays, respectively, and the other symbols have their usual meanings. To account for positron captures (ϵ^+) and β^+ decays one simply needs to change the sign of μ (the electron chemical potential including rest mass) in Eq. (4). The neutrino spectra have been calculated using Eq. (4) with the effective Q-values and effective rates (Langanke et al. 2001; Kunugise & Iwamoto 2007) with additional switching between capture and decay (Odrzywolek 2009). The above procedure reproduces neutrino fluxes and average neutrino energies of the original tabulated values at the FFN grid points. Between grid points, we used a bilinear interpolation of the effective rates and Q-values (Fuller et al. 1985). Electron chemical potential required in Eq. (4) has been computed separately with precision better than 1×10^{-12}.

2.2. Representative SN Ia explosion models

For the neutrino explosion diagnostic analysis, we have selected two representative explosion models from our database (Plewa 2007): a pure deflagration, n7d1r10t15c, and a delayed detonation, Y12. Both models were obtained for a standard carbon/oxygen Chandrasekhar mass white dwarf. A slightly modified flame capturing method of Khokhlov (1995) was used to follow a deflagration, and we used a 13 isotope alpha-network to directly compute energetics of the detonation wave. Both models are relatively energetic with explosion energies between ≈ 0.97 foe (1 foe = 1×10^{51} ergs) for the pure deflagration and ≈ 1.36 foe for the delayed-detonation.

2.3. Detailed analysis of the neutrino emission

For the selected explosion models, we have computed neutrino emission resulting from pair annihilation, plasmon decay and weak nuclear processes. The results are presented in the form of emissivity maps and total fluxes. Additionally, we provide time dependent neutrino energy spectra in numerical form (see Online Materials). Following practice known from core-collapse supernova studies, we show individual neutrino emission light curves for electron neutrinos (ν_e), electron antineutrinos ($\bar{\nu}_e$) and the average of the remaining four muon and tau neutrinos (ν_μ). The latter are produced exclusively in thermal processes, as long as we neglect neutrino oscillations. Electron neutrino (ν_e) flux is dominated either by electron captures on protons and iron group nuclei [3] (when the burning is the most intense) or pair annihilation (otherwise).

Electron antineutrinos ($\bar{\nu}_e$) are produced mainly in the pair process and through positron captures on neutrons. Heavy nuclei (β^- decays and e^+ captures) do not contribute to the total $\bar{\nu}_e$ flux significantly. Muon and tau neutrinos are produced in much smaller quantities only in the thermal processes, and one may expect that actually more μ/τ neutrinos are produced due to flavor conversion between source and detector (see Fig. 3 in Kunugise & Iwamoto (2007)). Plasmon decay is almost negligible due to low densities, and low energy of the emitted neutrinos (~few keV, Odrzywołek 2007) makes their detection essentially impossible.

2.3.1. Pure deflagration model

Pure deflagrations produce neutrino emission with a single maximum (since explosion involves only one stage), and nuclear burning takes $\approx$ 1 second. We calculate the total neutrino flux (Fig. 1d) as the sum of thermal and weak components. The evolution is slower compared to a detonation (see below), and in this case therefore neutrino cooling processes are given more time compared to a detonation. Moreover, larger volume is involved in neutrino cooling in deflagration compared to a "failed" case, Y12 (cf. Fig. 2 versus Fig. 4). Overall neutrino luminosity is much larger compared to Y12 model and reach 1.92×10^{50} erg/s, almost order of magnitude larger compared to first peak luminosity of the Y12 model (1.1×10^{49} erg/s). Total energy radiated in neutrinos is 0.04 foe, five times more than for Y12 (0.008 foe) but still small compared to overall explosion energy of $\approx$ 1 foe.

Temporal evolution of the neutrino emission in the deflagration model are shown in Fig. 1a (ν_e), Fig. 1b ($\bar{\nu}_e$), Fig. 1c (ν_μ), with the total neutrino luminosity shown in Fig. 1d. Overall, the emission varies smoothly in time and we notice only very small emission fluctuations. Even though the flame is geometrically very convoluted (Fig. 2), the neutrino emission is produced in regions of nearly identical density and temperature. We found that most (99%) of the NSE neutrino flux is produced for $T_{NSE} < T_9 < 10$ and $8.9 < \log_{10}\rho < 9.3$. At the peak neutrino emission, only 3% of the total white dwarf mass is emitting neutrinos.

We note that the model neutrino emission obtained in our axisymmetric deflagration is very similar to that of the spherically symmetric model W7 (Nomoto et al. 1984, 1993; Kunugise & Iwamoto 2007). This hints that the neutrino emission from pure deflagrations may have a generic form. To verify this impression, we have computed the neutrino light curves for two other deflagration models presented by (Plewa 2007), n11d2r10t15a and n11d2r20t20b. In both cases the neutrino emission displayed very similar characteristics to W7 and the deflagration model analyzed in detail here. The generic form of the emission also implies that *neutrinos may not provide information helpful in differentiating between various scenarios of pure deflagrations*.

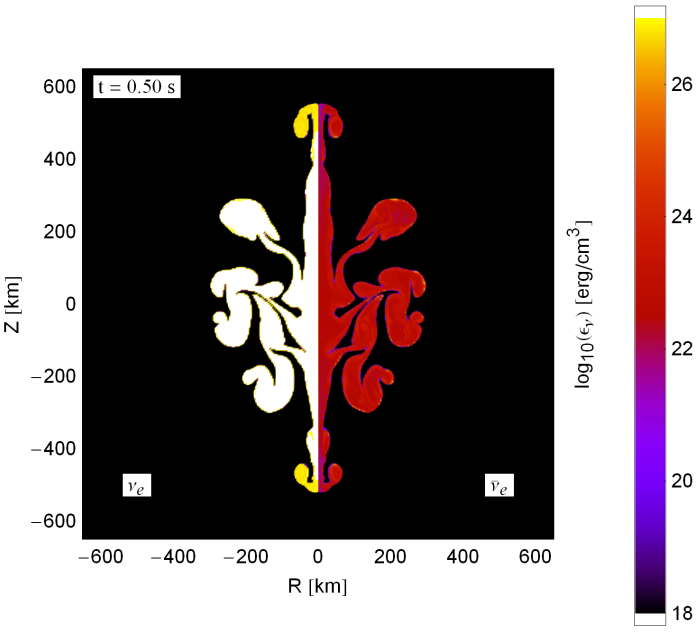

Fig. 2. Maps of the neutrino emissivity in the pure deflagration model at $t = 0.5$ s (i.e. near the peak of the neutrino emission). (left segment, $R < 0$ km) ν_e; (right segment, $R > 0$ km) $\bar{\nu}_e$.

[3] Especially ^{55}Co and ^{56}Ni.

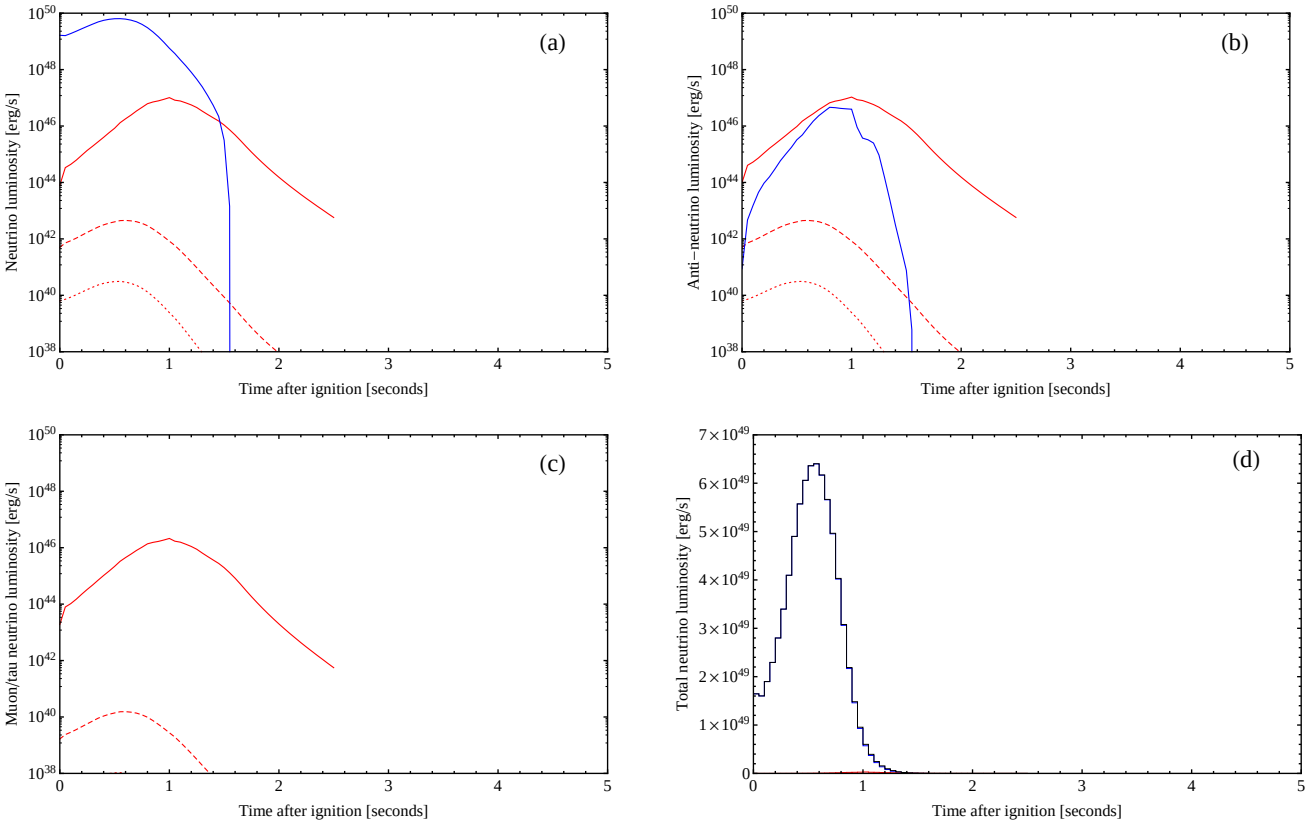

Fig. 1. Model neutrino luminosities of the pure deflagration n7d1r10t15c. (a) electron neutrinos, L_{ν_e}; (b) electron anti-neutrinos, $L_{\bar{\nu}_e}$; (c) μ and τ neutrinos, $L_{\bar{\nu}_x}$; (d) total flux. In each panel we show the contribution of weak (solid blue, Eq. (2)), pair annihilation (solid red, Eq. (1a)), transverse (dashed red) and longitudinal (red dotted) plasmon decay (Eq. (1b)).

2.3.2. Delayed-detonation model

In contrast to the pure deflagrations delayed detonation class of models produce multi-peak neutrino emission. The two distinct neutrino emission maxima due to initial deflagration stage and delayed detonation can be clearly discerned (Fig. 3). Deflagration peak is completely dominated by the ν_e emission due to electron captures. Detonation peak while still dominated by the weak nuclear processes, includes significant fraction of the thermal emission. Actually, pair annihilation dominates after end of rapid detonation stage and form an exponentially decaying tail. This is result of the efficient neutrino cooling in the large volume of the former white dwarf swept by the detonation wave (cf. Fig. 5).

Electron flavor neutrino and antineutrino emission maps (Figs. 4 and 5) reflect the explosion physics. Roughly speaking, neutrino emission is a by-product of the thermonuclear flame or the detonation wave. During the deflagration stage, almost all ν_e's are emitted in the electron capture processes in the region swept by the thermonuclear flame. Hot plumes expanding into the higher density gas are prominent sources of electron neutrinos, because electron capture rates are increasing rapidly with the temperature (due to thermal population of excited states with large matrix elements) and density (due to Fermi energy crossing capture threshold for excited nuclei). Total mass involved in neutrino emission is much smaller than for pure deflagration model, 0.2% of the total white dwarf mass.

Antineutrinos ($\bar{\nu}_e$) are emitted from much larger volume heated by the thermonuclear burning. Electron antineutrino emission from thermal processes (pair annihilation) during the deflagration stage is initially suppressed due to high degeneracy of the electron gas. The main source of $\bar{\nu}_e$'s is pair annihilation

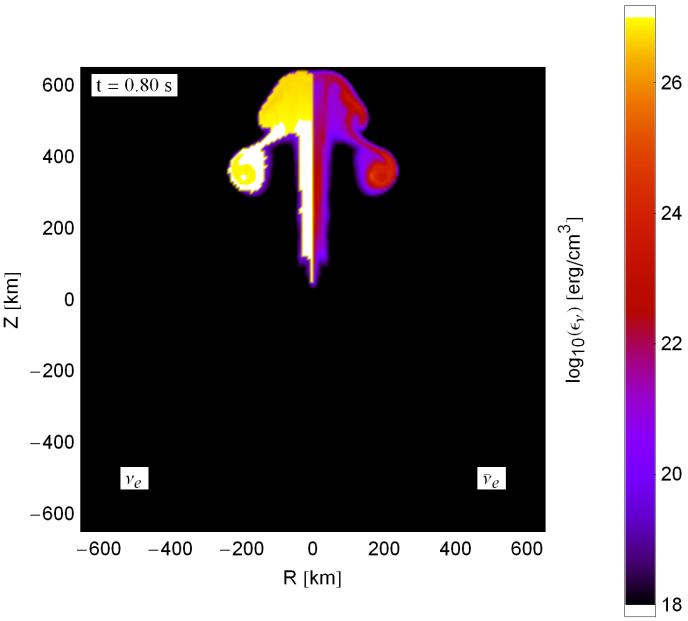

Fig. 4. Maps of the neutrino emissivity in the delayed-detonation model at t=0.8 s (i.e. near the peak of the neutrino emission produced by the initial failed deflagration stage). (left segment, $R < 0$ km) ν_e; (right segment, $R > 0$ km) $\bar{\nu}_e$.

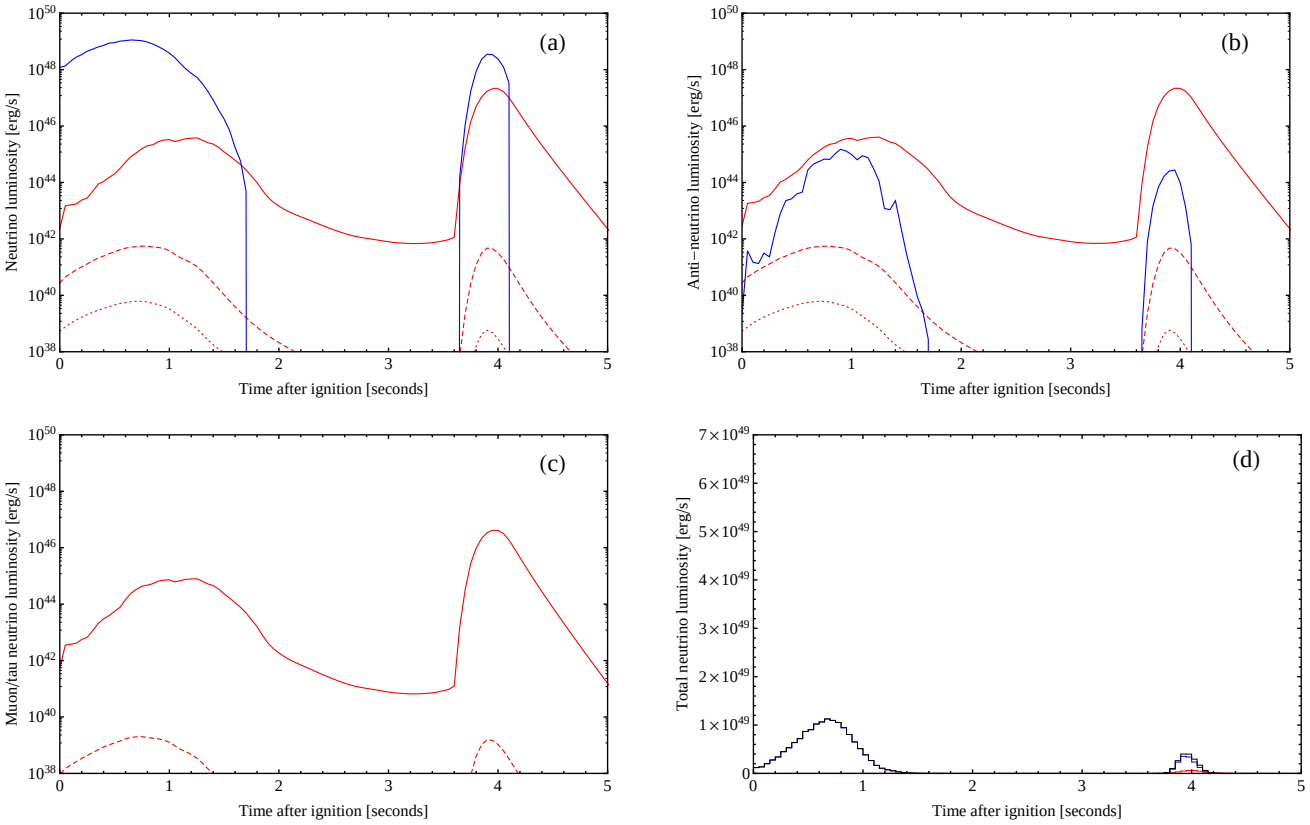

Fig. 3. Model neutrino luminosities of the delayed-detonation Y12. (a) electron neutrinos, L_{ν_e}; (b) electron anti-neutrinos, $L_{\bar{\nu}_e}$; (c) μ and τ neutrinos, $L_{\bar{\nu}_x}$; (d) total flux. The color and line-style coding is identical to that in Fig. 1.

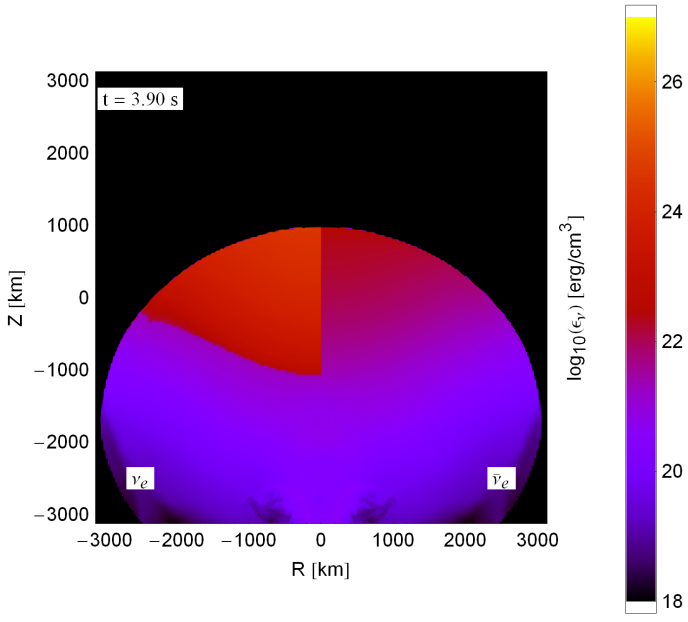

Fig. 5. Maps of the neutrino emissivity in the delayed-detonation model at t=3.9 s (i.e. near the peak of the neutrino emission produced by the detonation stage). (left segment, $R < 0$ km) ν_e; (right segment, $R > 0$ km) $\bar{\nu}_e$.

(Eq. (1a)) and the reaction

$$e^+ + n \rightarrow p + \bar{\nu}_e.$$

After $t \approx 1$ s, pair annihilation completely dominates the $\bar{\nu}_e$ flux (Fig. 3b, red solid curve).

Deflagration stage ends with a bubble breakout and the neutrino emission due to nuclear processes ceases. Thermal neutrinos are still emitted from area heated during nuclear burning, but the neutrino flux decreases by several orders of magnitude (see Figs. 3a-c). At $t = 3.7$ s, the material accelerated by the expanding bubble starts converging at the location opposite to the bubble breakout point, and eventually triggers a detonation. Interestingly, the thermal neutrino emission starts to rise just prior to the detonation ignition (Fig. 3c). This is due to the neutrino cooling of the colliding matter which heats up enough to produce e^+e^- pairs. Once the detonation[4] is formed, the wave quickly moves into the white dwarf core. The nuclear burning involves electron captures and weak nuclear neutrinos are the dominant component of the neutrino emission (left segment in Fig. 5).

In contrast to the pure deflagration, during the detonation phase a large fraction of the white dwarf ($\approx$ 30% in mass) is participating in producing the neutrino emission. We found that in this case $\approx$ 50% of the emission is produced by matter with $T_{NSE} < T_9 < 7.2$ and $7.85 < \log_{10}\rho < 8.25$. Thermal neutrinos are also emitted from much larger volume (of the deflagration-expanded white dwarf) swept by the detonation (see right panel in Fig. 5), and are the main contributor to the $\bar{\nu}_e$ flux. Only residual pair neutrino emission from the deflagration stage can still be seen at this time. Once the detonation ends, however, the ejecta

[4] The detonation is a reactive wave in which a thin hydrodynamic shock activates thermonuclear burn and is followed by an extended post-shock region in which the thermonuclear fuel is processed and the energy is released (Fickett & Davis 1979).

quickly expand and cool down adiabatically, and the supernova becomes an exponentially fading source of thermal neutrinos[5].

2.3.3. Comparison of neutrino emission signatures

One of the most exciting possibilities opened by the neutrino channel is a potential for differentiating between various explosion scenarios. While the overall number of scenarios is quite large, most of them fit into either a pure deflagration or a delayed-detonation category. Therefore, two models analyzed in previous sections provide a small but representative sample. We have at least three observables available for the explosion diagnostics: total energy radiated by neutrinos (directly related to the observed number and energy of events), time variation of the neutrino signal (sensitive to the burning speed and burning type), and the energy of detected neutrinos (probing the degeneracy of the burning matter). Analyzed models differ in these three respects quite significantly (see Table 1). The most striking difference is the total emitted neutrino energy which almost entirely comes from the electron flavor neutrino. The delayed-detonation model produces five times less energy in neutrinos despite comparable explosion energy. Therefore, in case of the nearby explosion unobscured by an interstellar matter we can easily identify explosion scenario provided the total (kinetic+radiative) explosion energy can be determined. Neutrino energies are also a little bit smaller in the delayed-detonation model (Table 1). Unfortunately, only ν_e provide clear signature. Other neutrino flavors, including relatively easy to detect $\bar{\nu}_e$'s, are emitted in comparable quantities. The total energy radiated in $\bar{\nu}_\mathrm{e}$ is $\approx 7.0\times10^{46}$ erg for n7d1r10t15c, comparable to $\approx 6.2\times10^{46}$ ergs for Y12. Average $\bar{\nu}_\mathrm{e}$ energy in the case of Y12 model (3.5 MeV) is only 0.3 MeV lower compared to a pure deflagration (3.8 MeV).

The characteristic double-peaked neutrino luminosity curve (Fig. 3) is a "smoking gun" of the delayed-detonation supernova, although the second maximum is rather weak. However, due to $\approx$ 4 seconds delay between the maxima, and compared to $\approx$ 2.5 seconds long deflagration, a detection of a neutrino events a few seconds apart would offer evidence for the explosion due to a delayed detonation.

3. Discussion

3.1. Prospects for neutrino detection from a galactic Type Ia supernova

In the context of SN Ia neutrino emission, possibly the most important question is whether the supernova neutrino signal can be measured using the available neutrino-detection technologies. To answer this question one requires the following information: (1) estimated galactic supernova rates and expected supernova distances, (2) the integrated supernova neutrino (ν_e) and antineutrino ($\bar{\nu}_e$) spectra; (3) characteristics of suitable neutrino detector. In the following discussion we will consider a supernova located at the distance of 1 kpc[6]. The results for a widely adopted 10 kpc distance (roughly a distance to the Galactic Center with the corresponding volume including ≈50% stars in the Milky Way, Bahcall & Soneira 1980) can be obtained by dividing the current numbers by a factor of 100.

The selection of the interesting nuclei and processes of interest is potentially quite complicated due the large number of the nuclei involved in NSE neutrino emission, each with unique (often not well-known) spectral properties, and contribution from additional thermal processes. To aid the selection process, we construct a diagram showing the temporal evolution of neutrino emission from individual nuclides and/or processes integrated over the stellar volume as a function of the neutrino energy.[7] Specifically, we plot $(\langle\mathcal{E}_\nu\rangle(t), F_\nu(t))$ on the F_ν-$\langle\mathcal{E}_\nu\rangle$ plane. This diagram might be referred to as the ν-HR diagram, with the mean neutrino energy considered an analogue of the effective stellar temperature and the neutrino flux now playing a role of the stellar bolometric luminosity. For a given supernova distance and detector, once can also show isocontours of detection rates. Since the knowledge of the mean neutrino energy and integrated flux is not enough to reproduce the energy spectrum, in calculating detection rates we are forced to assume a single parameter spectral function. In neutrino astrophysics, it is common to use the Fermi-Dirac function (Kiełczewska 1990):

$$\Phi(\mathcal{E}_\nu, t) \equiv \frac{R(t)}{\langle\mathcal{E}_\nu\rangle(t)^3}\frac{a\,\mathcal{E}_\nu^2}{1+e^{b\,\mathcal{E}_\nu/\langle\mathcal{E}_\nu\rangle}} \quad a\approx 17.3574,\ b\approx 3.15137, \tag{5}$$

where, $R(t)$, the integrated particle emission rate and, $\langle\mathcal{E}_\nu\rangle(t)$, the average neutrino energy depend only on time, and a and b normalize the spectrum.

For the assumed supernova distance of 1 kpc, the results for a pure deflagration model and a Super-Kamiokande class detector (H_2O target with Cherenkov light detector with threshold of 4 MeV) are shown in Fig. 6. In particular, the following can be concluded from the results shown in Fig. 6:

(1) the most important nuclei in both flux and induced in Super-Kamiokande-like detector events terms are free protons and ^{55}Co; expected event rate is in 1 kt of H_2O up to 0.1/sec: as explosion takes ≈1 second in Super-Kamiokande we expect up to $0.1/s/kt\times 32kt\times 2\mathrm{nuclei}\approx 6$ events from 1 kpc;
(2) secondary source of detectable signal are: ^{56}Ni, ^{56}Co, ^{53}Fe and ^{54}Co with mean energies of ≈ 3 MeV, ≈ 4 MeV, ≈ 6 MeV, and ≈ 9 MeV, respectively;
(3) numerous other nuclei as well as thermal processes produce either a weak or undetectable signal.

Note that in Fig. 6 the evolution proceeds along curves from high energy to low energy neutrinos (i.e. from right to left). This is opposite to core-collapse supernova neutrinos.

The results of similar analysis for antineutrinos from the delayed-detonation model, Y12, are shown in Fig. 7. We consider the inverse beta decay ($\bar{\nu}_\mathrm{e} + p \rightarrow n + e^+$) as the detection channel, and a Gd-loaded water Cherenkov detector proposed by Beacom & Vagins (2004) or a liquid scintillator detector, e.g. KamLAND (Eguchi et al. 2003). We note that here the detection method is simply the inverse of the essential production process ($e^+ + n \rightarrow p + \bar{\nu}_\mathrm{e}$). Analysis of Fig. 7 leads to the following conclusions:

(1) the most important for $\bar{\nu}_\mathrm{e}$ emission processes are pair-annihilation and positron capture on neutrons
(2) weak nuclear processes from nuclei are on level of being negligible
(3) expected event rate is very small (~few mHz/kt@1 kpc); at least a half megaton detector is required to observe a single event from 1 kpc

[5] See http://ribes.if.uj.edu.pl/snIa/ for step-by-step neutrino emissivity maps, animations, digitized neutrino spectra, and additional data.

[6] Before SN 1987A, it was not unusual to adopt a 1 kpc distance to the "future core-collapse supernova;" see, e.g., Burrows (1984).

[7] Similar diagrams can be used to discuss other phenomena, e.g. evolution of pre-supernovae (Odrzywolek 2007).

Table 1. Integrated properties of the model neutrino signals.

Model	n7d1r10t15c	Y12 (def)	Y12 (det)	Y12 (total)
E_ν^{total} [erg]	3.85×10^{49}	7.3×10^{48}	8.7×10^{47}	8.2×10^{48}
$E_\nu^{total}/E_{nucl}^{total}$	0.03	0.05	0.0005	0.004
$E_{\nu_e}^{total}$ [erg]	3.85×10^{49}	7.3×10^{48}	7.7×10^{47}	8.05×10^{48}
$E_{\bar{\nu}_e}^{total}$ [erg]	7.0×10^{46}	8.9×10^{45}	5.9×10^{46}	6.8×10^{46}
$E_{\nu_x}^{total}$ [erg]	6.4×10^{46}	2.2×10^{45}	4.4×10^{46}	4.6×10^{46}
$\langle \mathcal{E}_{\nu_e} \rangle^{total}$ [MeV]	3.8	3.7	2.35	3.5
$\langle \mathcal{E}_{\bar{\nu}_e} \rangle^{total}$ [MeV]	2.9	3.0	1.9	2.0
$\langle \mathcal{E}_{\nu_x} \rangle^{total}$ [MeV]	2.5	2.8	2.0	2.0
double L_ν peaks	no	peak 1	peak 2	yes
signal duration [s]	1.0	1.0	0.4	separation ~3 sec

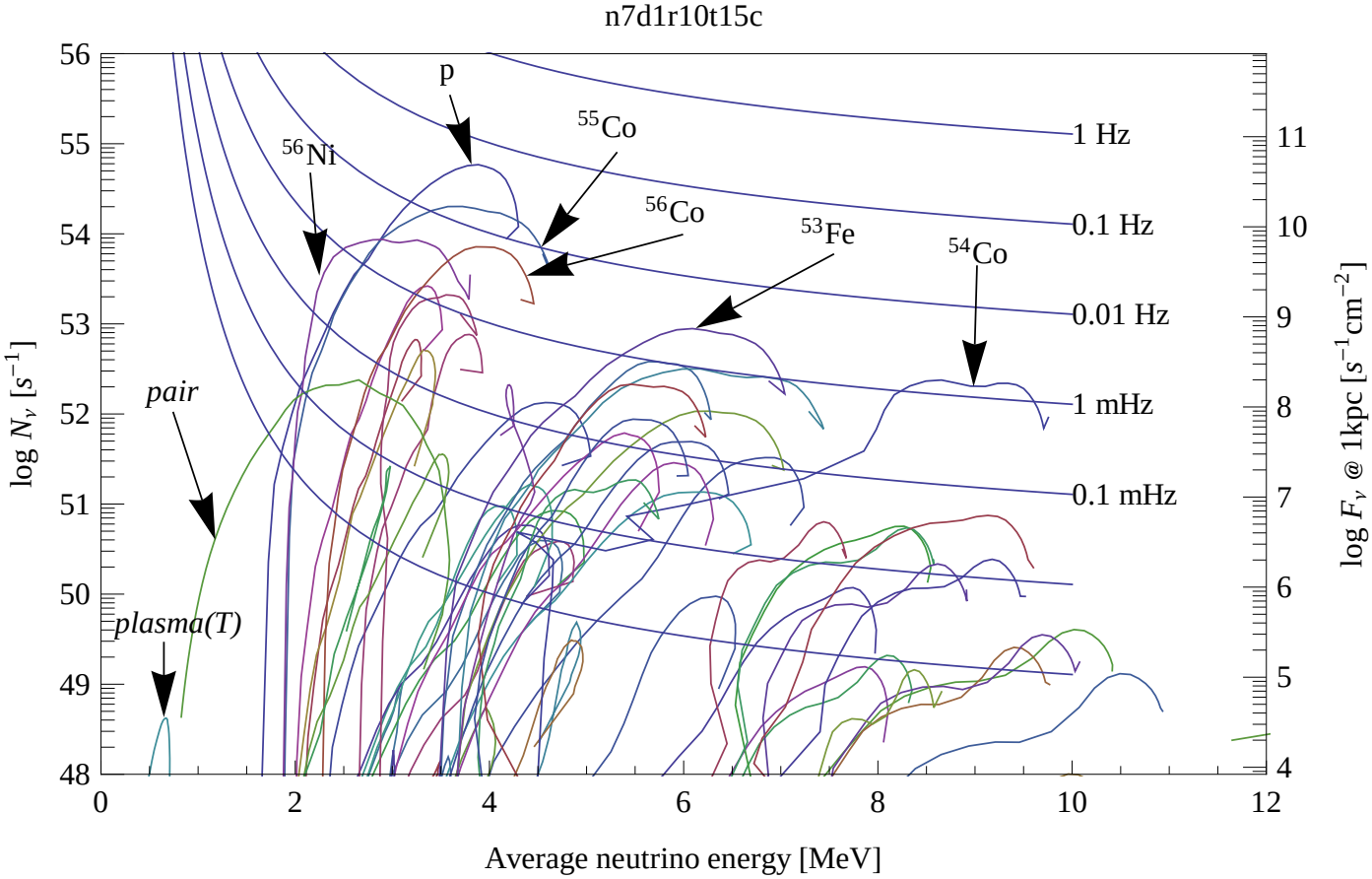

Fig. 6. Neutrino-HR diagram for n7d1r10t15c model. Every curve is a track on a $F_{\nu_e} - \langle \mathcal{E}_{\nu_e} \rangle$ plane produced by single nucleus/ thermal process. Assuming a single parameter neutrino energy spectrum (Eq. (5)), we are able immediately select the most interesting for further analysis processes and estimate the expected signal in a given neutrino detection channel. Particularly, we have presented detection of ν_e using elastic scattering off electrons with threshold for detection of the electron kinetic energy of 4 MeV in water Cherenkov detector.

Following the analysis of ν_e,$\bar{\nu}_e$ detection in other cases, we selected five the most promising SN Ia neutrino experiments:

1. IBD2: inverse beta decay $\bar{\nu}_e + p \rightarrow n + e^+$ utilized in large 50 kiloton target liquid scintillator detector (e.g. LENA Autiero et al. 2007; Marrodán-Undagoitia et al. 2006; Oberauer et al. 2005) or Gd-loaded water detector (Beacom & Vagins 2004) with 1.8 MeV threshold
2. ES0: elastic scattering off electrons $\nu_e + e^- \rightarrow \nu_e + e^-$ in large 50 kt liquid scintillator (LENA) assuming ≈0.2 MeV threshold
3. ES4: elastic scattering off electrons $\nu_e + e^- \rightarrow \nu_e + e^-$ in extremely large water Cherenkov detector Memphys (Autiero et al. 2007; Rubbia 2009), Titan-D (Suzuki 2001, 2008; Kistler et al. 2008), LBNE W.C. (Scholberg 2010) etc. assuming standard 4.0 MeV detection threshold for recoil electrons
4. LAr: neutrino absorption in 100 kt of liquid argon (see e.g. Rubbia 2009, GLACIER proposal) detected using coincidence of electrons and delayed gammas ($\nu_e + {}^{40}\mathrm{Ar} \rightarrow {}^{40}\mathrm{K}^* + e^-$, Raghavan 1986) and elastic scattering off electrons ($E_{\mathrm{th}} = 5$ MeV)

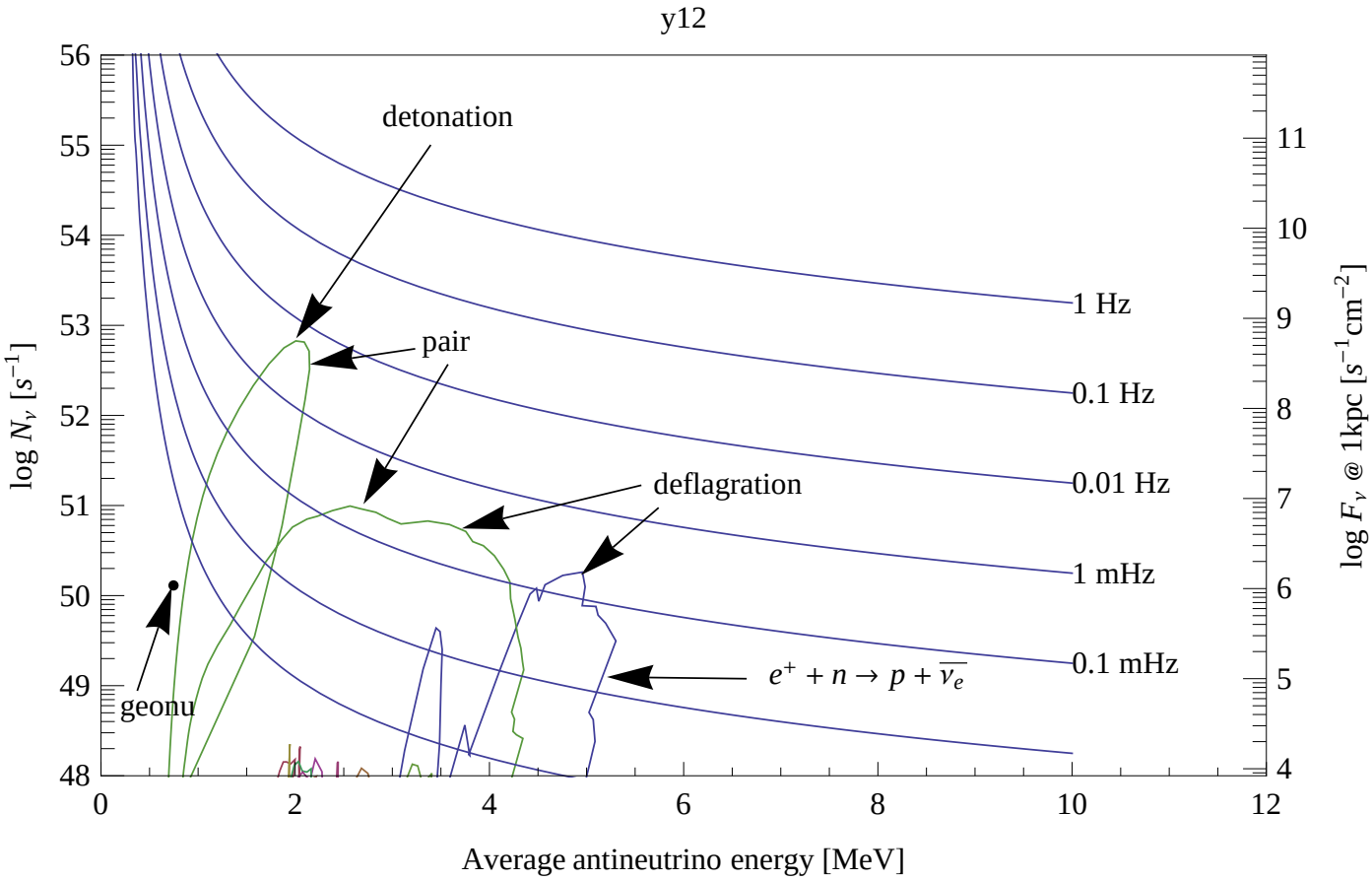

Fig. 7. Anti-neutrino-HR diagram for Y12 model. Similar to Fig. 6, but now we consider detection of $\bar{\nu}_e$ *via* inverse beta decay in $GdCl_3$-loaded H_2O with threshold of 2 MeV.

5. PES: elastic scattering off protons in advanced extremely low background liquid scintillator detector like Borexino (Alimonti et al. 2009)
6. COS: coherent elastic scattering off high A nuclei (e.g. ^{72}Ge) in detector with threshold of the order of 100 eV

While scenarios IBD2, ES0, ES4, and LAr use a proven technology (Fulgione 2010), proton elastic scattering (PES) and neutrino-nucleus coherent scattering (COH) have never been used in practice for low ν energy. However, from theoretical analysis and preliminary experimental results we expect to observe significant progress in development of neutrino detectors. Besides possible gains due development of advanced detection methods, larger target masses are required for successful detection of SN Ia neutrinos in the foreseeable future.

Table 2 shows the expected number of neutrino events for prospective neutrino experiments. In case of a delayed-detonation, we have separated contributions from the initial deflagration and the following delayed detonation. For weak neutrinos and antineutrinos, the total number of expected events is simply the sum of events produced in individual explosion stages. For thermal neutrinos, there is also a minor contribution from the neutrinos emitted during the period separating the two explosion stages and during the final expansion stage. Clearly, the largest yield is due to the ν_e emission from electron captures during the deflagration stage. This is expected since the neutrino luminosity is dominated by these neutrinos and reaches $1.1{\times}10^{49}$ erg/s for delayed-detonation and 6.4×10^{49} for pure deflagration. Finally, the time delay between the two emission maxima of a delayed-detonation SN and their relative length will be very important aspects of the data analysis.

3.1.1. Neutrino background and signal-to-noise ratio

Additional comments on the expected background signals are due. In the case of ν_e emission and supernova at larger (>10 kpc) distance, we face a problem of the background emission from ^{8}B, ^{7}Be and CNO solar neutrinos (left panel in Fig. 8). Here a directional detection could be a solution, but no practical method of this kind exists. Electron antineutrino emission will be blended with the geoneutrinos (Fig. 8, right) and the terrestrial nuclear power plants. The geoneutrino flux varies slightly across continental crust and is much smaller on the ocean floor (Learned et al. 2006; Araki et al. 2005; BOREXINO Collaboration et al. 2010). Flux from human-made sources strongly depends on the location of the detector and vary in time (Lasserre & Sobel 2005). Other sources of neutrinos, e.g. from cosmological core-collapse supernovae[8] (flux $\ll 10$ cm^{-2} s^{-1}, Lien et al. 2010, Totani & Sato 1995; dot-dashed curve in the right panel of Fig. 8) are far below the expected signal from a galactic SN Ia. Relic neutrino flux is of the order of $56\,c \simeq 1\times10^{12}$ cm^{-2} s^{-1}, but the energy is very small in this case ($\sim 10^{-4}$ eV).

[8] Those supernovae are a source of the Diffuse Supernova Neutrino Background (Horiuchi et al. 2009). The fact that the sky is relatively dark in $\bar{\nu}_e$, compared to individual sources, is the neutrino version of the Olbers paradox.

Table 2. Expected number of events triggered in the select proposed neutrino detectors by a thermonuclear supernova located at a distance of 1 kpc.

detector	n7d1r10t15c deflagration 0-2.5s	Y12 deflagration 0-2s	Y12 detonation 3.5-4.5s	Y12 total 0-7s	proposals	status
ES4 (0.5 Mt)	19	3.2	0.1	3.3	Hyper-Kamiokande, Memphys	under construction
LAr (100 kt)	21.4 + 1.5	3.8+0.24	0.08+0.005	3.9+0.25	Glacier	under construction
IBD2 (50 kt)	0.2	0.01	0.06	0.07	Gadzooks!, LENA	proposed
ES0 (50 kt)	14	2.7	0.26	2.9	LENA	proposed
PES (50 kt)	60	11.1	0.8	12.0	LENA	proposed
COH (1000 kg)	0.03	0.005	0.0003	0.006	-	planned

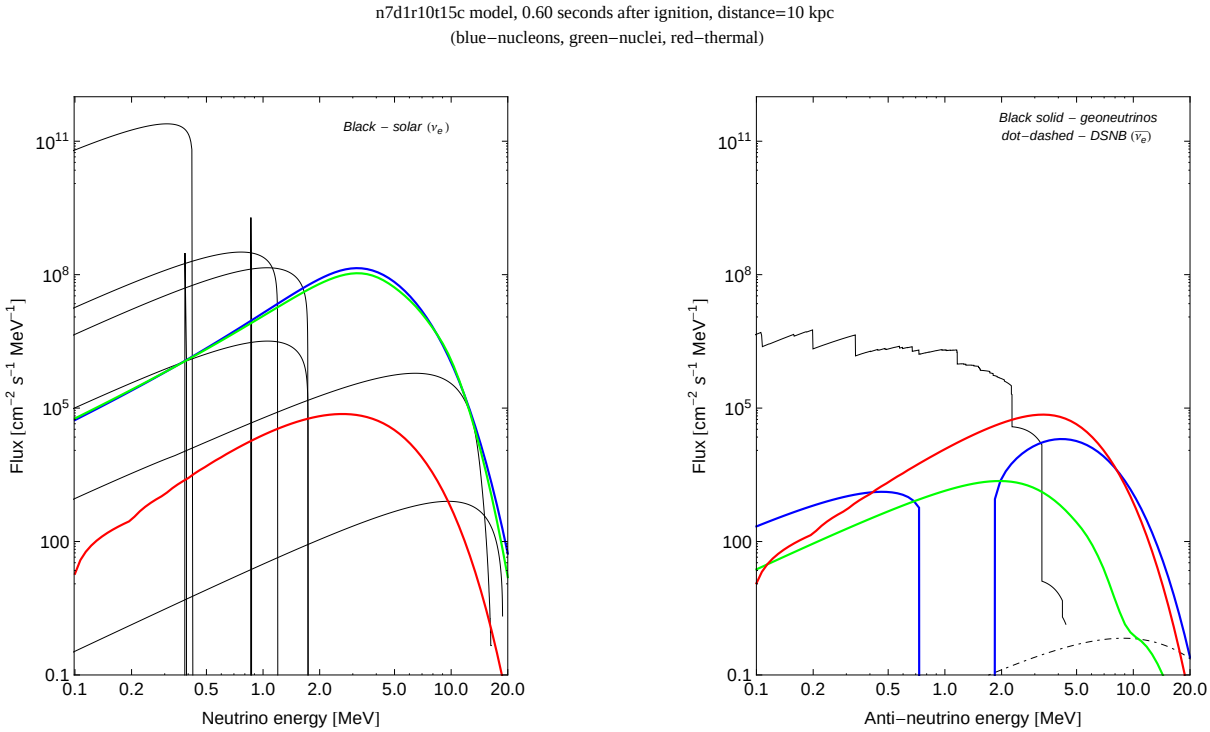

Fig. 8. The ν_e (left) and $\bar{\nu}_e$ (right) model spectra of a pure deflagration supernova near the maximum of the neutrino emission and other recently studied sources. The supernova emission level is for an event located at a distance $d = 10$ kpc. References for the data used: solar neutrinos, Bahcall et al. (2005); geoneutrinos at Kamioka, Japan, Enomoto (2005, 2006); DSNB, Lien et al. (2010).

From Fig. 8 it is clear that the neutrinos from a galactic SN Ia could be detected, especially for the pure deflagration event. Neutrino observations of such a supernova is mainly a technological challenge (requires very large detector mass, new detection techniques, low energy threshold, etc.) and, similar to SN 1987A, a matter of chance. Cappellaro et al. (1997) estimated that 4 ± 1 Type Ia supernovae per millennium for Galaxy. An Earth-centered ball with the radius of 10 kpc (1 kpc) contains $\approx 50\%$ ($\approx 0.5\%$) of stars (Bahcall & Soneira 1980), and the corresponding SN Ia explosion probability within a period of 10 years is therefore ≈ 0.02 ($\approx 2 \times 10^{-4}$).

4. Conclusions

We have obtained and analyzed neutrino light curves and neutrino spectra for two models of the most popular Type Ia supernova explosion scenarios: a pure deflagration and a delayed detonation. We have discussed the role of physical conditions in producing neutrinos in these types of explosions. In particular, the neutrino emission studies allow to directly probe the density, temperature, and composition of the neutrino-emitting matter. This motivates development of neutrino experiments to explore stellar evolution physics beyond core-collapse supernova and solar applications.

Due to their cosmological importance and with their exact origins remaining unknown, thermonuclear supernovae are one class of exciting future targets of the neutrino astronomy. The upcoming challenge is a detection of the SN Ia neutrinos. Several recently proposed neutrino experiments will offer sensitivity that will allow for detecting a thermonuclear event at kpc distances. More importantly, we find the that *the next generation of neutrino detectors will be able to unambiguously identify the mechanism responsible for the explosion*. In particular, SN Ia supernova electron neutrinos probe the thermonuclear deflagration stage while the electron antineutrinos probe the detonation phase. As the electron neutrinos are almost exclusively due to electron captures associated with the thermonuclear flame, they offer means to study both nuclear and combustion physics under

extreme conditions. On the other hand, the delayed electron antineutrino signal provides direct evidence for thermonuclear detonation. Finally, the muon neutrinos are exclusively produced in thermal processes and could potentially be used to extract weak nuclear signal.

Given a relatively low neutrino luminosity of SN Ia events due to delayed detonations, their characteristic double-peaked neutrino light curves can be used to reduce the false alarm rate and serve as an early warning system for this type of events. A pure deflagration SN Ia produces only a single neutrino emission maximum with somewhat faster rise time compared to a delayed detonation. The predicted number of observed neutrino events is however higher for deflagrations thanks to both higher neutrino luminosity and slightly higher energies of the emitted neutrinos. For a 0.5 Mt classical water Cherenkov detector (LBNE WC, Long Baseline Neutrino Experiment Scholberg 2010; Memphys (Autiero et al. 2007; Rubbia 2009)), we predict recording about 20 elastic scattering events above 4 MeV per second for a SN Ia event located at a distance of 1 kiloparsec. Still larger detectors (e.g. Titan-D Suzuki 2001, 2008; Kistler et al. 2008) almost certainly guarantee positive detection of a galactic SN Ia. However, this holds true only for a pure deflagration; *the predicted neutrino fluxes for a delayed detonation are about 5 times lower making such events much harder to detect*. We also found that the neutrino emission is very similar in two-dimensional axisymmetric and spherically symmetric pure deflagration models (i.e. W7 by Nomoto et al. (1984)). This leads us to believe that *the neutrino observations will not help to distinguish between specific scenarios of pure deflagrations* (e.g. ignition occurring at a single point or at multiple points).

The majority of neutrino experiments considered here (detectors I, II, and IV in Table 2) use large amounts of a liquid scintillator. This type of experiments might be the most viable and successful in detecting Type Ia supernovae, especially if a proton elastic scattering (PES) method is utilized (Beacom et al. 2002). One example of such a device is the Borexino detector (Alimonti et al. 2009). Although perhaps too small for detecting a thermonuclear supernova at a kpc distance, Borexino will be an essential testbed for the proposed and much larger LENA (Autiero et al. 2007; Marrodán-Undagoitia et al. 2006; Oberauer et al. 2005) and other similar experiments (Maricic & the Hanohano collaboration 2010). We also note that neutrinos can be detected using neutrino-nucleus elastic scattering (Drukier & Stodolsky 1984; Giomataris et al. 2008; Collar 2010; Barbeau et al. 2003). However, a practical application of this technique to SN Ia may not be possible due to prohibitively large required mass of the detector.

We conclude that a significant progress in terms of neutrino detection methods is needed for the neutrinos to become a practical tool for studying Type Ia supernovae. However, a detection of a thermonuclear event at a distance of few kiloparsecs will be within the reach of the planned neutrino observatories and will offer a perfect chance to identify the mechanism driving the explosion.

Acknowledgements. We thank Thomas Janka for encouragement and helpful advice, and an anonymous referee for comments that helped improving the initial version of this paper. TP was supported through the DOE grant DE-FG52-03NA000064. This research used resources of the National Energy Research Scientific Computing Center, which is supported by the Office of Science of the U.S. Department of Energy under Contract No. DE-AC02-05CH11231, and NASA's Astrophysics Data System.

References

Ahmad, Q. R., Allen, R. C., Andersen, T. C., et al. 2001, Physical Review Letters, 87, 071301
Alekseev, E. N., Alekseeva, L. N., Volchenko, V. I., & Krivosheina, I. V. 1987, JETP Lett., 45, 589
Alimonti, G., Arpesella, C., Back, H., et al. 2009, Nuclear Instruments and Methods in Physics Research Section A: Accelerators, Spectrometers, Detectors and Associated Equipment, 600, 568
Ando, S., Beacom, J. F., & Yüksel, H. 2005, Physical Review Letters, 95, 171101
Araki, T., Enomoto, S., Furuno, K., et al. 2005, Nature, 436, 499
Arcones, A., Martinez-Pinedo, G., & Woosley, S. E. 2010, ArXiv e-prints
Arnett, D. 1996, Supernovae and Nucleosynthesis (Princeton: Princeton University Press)
Arnett, W. D., Bahcall, J. N., Kirshner, R. P., & Woosley, S. E. 1989, ARA&A, 27, 629
Arpesella, C., Back, H. O., Balata, M., et al. 2008, Physical Review Letters, 101, 091302
Aufderheide, M. B., Fushiki, I., Fuller, G. M., & Weaver, T. A. 1994a, ApJ, 424, 257
Aufderheide, M. B., Fushiki, I., Woosley, S. E., & Hartmann, D. H. 1994b, ApJS, 91, 389
Autiero, D., Äystö, J., Badertscher, A., et al. 2007, Journal of Cosmology and Astro-Particle Physics, 11, 11
Badenes, C., Hughes, J. P., Bravo, E., & Langer, N. 2007, ApJ, 662, 472
Bahcall, J. N. 1989, Neutrino Astrophysics (Cambridge: Cambridge University Press)
Bahcall, J. N., Serenelli, A. M., & Basu, S. 2005, ApJ, 621, L85
Bahcall, J. N. & Soneira, R. M. 1980, ApJS, 44, 73
Barbeau, P. S., Collar, J. I., Miyamoto, J., & Shipsey, J. 2003, IEEE Transactions on Nuclear Science, 50, 1285
Beacom, J. F., Farr, W. M., & Vogel, P. 2002, Phys. Rev. D, 66, 033001
Beacom, J. F. & Vagins, M. R. 2004, Phys. Rev. Lett., 93, 171101
BOREXINO Collaboration, Arpesella, C., Bellini, G., et al. 2008, Physics Letters B, 658, 101
BOREXINO Collaboration, Bellini, G., Benziger, J., et al. 2010, Physics Letters B, 687, 299
Bowden, N. S. 2008, Journal of Physics: Conference Series, 136, 022008
Braaten, E. 1991, Phys. Rev. Lett., 66, 1655
Braaten, E. & Segel, D. 1993, Phys. Rev. D, 48, 1478
Bruenn, S. W. 1985, ApJS, 58, 771
Burrows, A. 1984, ApJ, 283, 848
Burrows, A. 1990, Annual Review of Nuclear and Particle Science, 40, 181
Burrows, A. & Thompson, T. A. 2002, ArXiv Astrophysics e-prints
Cappellaro, E., Turatto, M., Tsvetkov, D. Y., et al. 1997, A&A, 322, 431
Caurier, E., Langanke, K., Martínez-Pinedo, G., & Nowacki, F. 1999, Nuclear Physics A, 653, 439
Clayton, D. D. 1984, Principles of Stellar Evolution and Nucleosynthesis (Chicago: The University of Chicago Press)
Cleveland, B. T. et al. 1998, Astrophys. J., 496, 505
Clifford, F. E. & Tayler, R. F. 1965a, MNRAS, 129, 104
Clifford, F. E. & Tayler, R. J. 1965b, MmRAS, 69, 21
Collar, J. I. 2010, Collar Group, Kavli Institute for Cosmological Physics, http://collargroup.uchicago.edu/
Drukier, A. & Stodolsky, L. 1984, Phys. Rev. D, 30, 2295
Dutta, S. I., Ratković, S., & Prakash, M. 2004, Phys. Rev. D, 69, 023005
Dye, S. E. 2006, Neutrino Geophysics : Proceedings of Neutrino Sciences 2005 (Springer Verlag)
Eguchi, K., Enomoto, S., Furuno, K., et al. 2003, Physical Review Letters, 90, 021802
Ellis, R. S., Sullivan, M., Nugent, P. E., et al. 2008, ApJ, 674, 51
Enomoto, S. 2005, PhD thesis, Tohoku University
Enomoto, S. 2006, Earth Moon and Planets, 99, 131
Esposito, S., Mangano, G., Miele, G., Picardi, I., & Pisanti, O. 2003, Nuclear Physics B, 658, 217
Fickett, W. & Davis, C. 1979, Detonation (Berkeley: University of California Press)
Fogli, G. L., Lisi, E., Mirizzi, A., & Montanino, D. 2005a, Journal of Cosmology and Astro-Particle Physics, 4, 2
Fogli, G. L., Lisi, E., Mirizzi, A., & Montanino, D. 2005b, Journal of Cosmology and Astro-Particle Physics, 4, 2
Fukuda, S. et al. 2001, Phys. Rev. Lett., 86, 5651
Fulgione, W. 2010, Journal of Physics: Conference Series, 203, 012077
Fuller, G. M., Fowler, W. A., & Newman, M. J. 1980, ApJS, 42, 447
Fuller, G. M., Fowler, W. A., & Newman, M. J. 1982a, ApJ, 252, 715
Fuller, G. M., Fowler, W. A., & Newman, M. J. 1982b, ApJS, 48, 279
Fuller, G. M., Fowler, W. A., & Newman, M. J. 1985, ApJ, 293, 1
Galeotti, P. et al. 1987, Helv. Phys. Acta, 60, 619
Gilfanov, M. & Bogdán, Á. 2010, Nature, 463, 924
Giomataris, I., Irastorza, I., Savvidis, I., et al. 2008, Journal of Instrumentation, 3, P09007

Guillian, E. H. 2006, Earth, Moon and Planets, 99, 309
Hachisu, I., Eriguchi, Y., & Nomaoto, K. 1986, ApJ, 308, 161
Hampel, W. et al. 1999, Phys. Lett., B447, 127
Han, Z. 1998, MNRAS, 296, 1019
Han, Z. & Podsiadlowski, P. 2004, MNRAS, 350, 1301
Hirata, K. et al. 1987, Phys. Rev. Lett., 58, 1490
Höflich, P. & Stein, J. 2002, ApJ, 568, 779
Horiuchi, S., Beacom, J. F., & Dwek, E. 2009, Phys. Rev. D, 79, 083013
Hoyle, F. & Fowler, W. A. 1960, ApJ, 132, 565
Iben, Jr., I. & Tutukov, A. V. 1984, ApJS, 54, 335
Immler, S., Weiler, K., & McCray, R. 2007, in American Institute of Physics Conference Series, Vol. 937, Supernova 1987A: 20 Years After: Supernovae and Gamma-Ray Bursters, ed. S. Immler, K. Weiler, & R. McCray
Isern, J., Bravo, E., Canal, R., & Labay, J. 1993, in Nuclei in the Cosmos 2, ed. F. Kaeppeler & K. Wisshak, 569–574
Itoh, N., Hayashi, H., Nishikawa, A., & Kohyama, Y. 1996a, ApJS, 102, 411
Itoh, N., Mutoh, H., Hikita, A., & Kohyama, Y. 1992, ApJ, 395, 622
Itoh, N., Nishikawa, A., & Kohyama, Y. 1996b, ApJ, 470, 1015
Iwamoto, K., Brachwitz, F., Nomoto, K., et al. 1999, ApJS, 125, 439
Iwamoto, K. & Kunugise, T. 2006, in American Institute of Physics Conference Series, Vol. 847, Origin of Matter and Evolution of Galaxies, ed. S. Kubono, W. Aoki, T. Kajino, T. Motobayashi, & K. Nomoto (New York: AIP), 406–408
Juodagalvis, A., Langanke, K., Hix, W. R., Martinez-Pinedo, G., & Sampaio, J. M. 2009, ArXiv e-prints
Kantor, E. M. & Gusakov, M. E. 2007, MNRAS, 381, 1702
Keil, M. T., Raffelt, G. G., & Janka, H.-T. 2003, ApJ, 590, 971
Kessler, R., Becker, A. C., Cinabro, D., et al. 2009, ApJS, 185, 32
Khokhlov, A. M. 1989, MNRAS, 239, 785
Khokhlov, A. M. 1991, A&A, 245, 114
Khokhlov, A. M. 1995, ApJ, 449, 695
Kiełczewska, D. 1990, Phys. Rev. D, 41, 2967
Kistler, M. D., Yuksel, H., Ando, S., Beacom, J. F., & Suzuki, Y. 2008, ArXiv e-prints
Kohyama, Y., Itoh, N., Obama, A., & Hayashi, H. 1994, ApJ, 431, 761
Kuhlen, M., Woosley, S. E., & Glatzmaier, G. A. 2006, ApJ, 640, 407
Kunugise, T. & Iwamoto, K. 2007, Publications of the Astronomical Society of Japan, 59, L57
Kutschera, M., Odrzywołek, A., & Misiaszek, M. 2009, Acta Physica Polonica B, 40, 3063
Langanke, K. & Martínez-Pinedo, G. 2000, Nuclear Physics A, 673, 481
Langanke, K., Martínez-Pinedo, G., & Sampaio, J. M. 2001, Phys. Rev. C, 64, 055801
Lasserre, T. & Sobel, H. W. 2005, Comptes Rendus Physique, 6, 749
Learned, J. G. 2004, White paper on Gigaton Array
Learned, J. G. 2005, Nuclear Physics B - Proceedings Supplements, 143, 152
Learned, J. G., Dye, S. T., & Pakvasa, S. 2006, Earth Moon and Planets, 99, 1
Leonard, D. C. 2009, Seeking Core-Collapse Supernova Progenitors in Pre-Explosion Images, arXiv:0908.1812v1 [astro-ph.SR]
Lhuillier, D. 2009, Nuclear Physics B - Proceedings Supplements, 188, 112 , proceedings of the Neutrino Oscillation Workshop
Lien, A., Fields, B. D., & Beacom, J. F. 2010, Phys. Rev. D, 81, 083001
Maricic, J. & the Hanohano collaboration. 2010, Journal of Physics: Conference Series, 203, 012137
Marrodán-Undagoitia, T., von Feilitzsch, F., Goeger-Neff, M., et al. 2006, Progress in Particle and Nuclear Physics, 57, 283 , international Workshop of Nuclear Physics 27th course - Neutrinos in Cosmology, in Astro, Particle and Nuclear Physics
Meng, X. & Yang, W. 2010, ApJ, 710, 1310
Misiaszek, M., Odrzywolek, A., & Kutschera, M. 2006, Phys. Rev. D, 74, 043006
Munakata, H., Kohyama, Y., & Itoh, N. 1985, ApJ, 296, 197
Nabi, J. & Klapdor-Kleingrothaus, H. V. 1999, Atomic Data and Nuclear Data Tables, 71, 149
Nabi, J.-U. & Sajjad, M. 2008, Phys. Rev. C, 77, 055802
Nakahata, M. 2007, Super-Kamiokande, http://sn1987a-20th.physics.uci.edu/0830-Nakahata.pdf
Nakahata, M. and Sobel, H. 2007, Twenty Years after SN1987A. What did we learn, what will the next Supernova teach us?, http://sn1987a-20th.physics.uci.edu/
Nomoto, K., Iwamoto, K., Nakasato, N., et al. 1997, Nuclear Physics A, 621, 467
Nomoto, K., Iwamoto, K., Tsujimoto, T., & Hashimoto, M. 1993, in Frontiers of Neutrino Astrophysics, ed. Y. Suzuki & K. Nakamura (Tokyo: Universal Academy Press), 235–254
Nomoto, K., Sugimoto, D., & Neo, S. 1976, Ap&SS, 39, L37
Nomoto, K., Thielemann, F.-K., & Yokoi, K. 1984, ApJ, 286, 644
Oberauer, L., von Feilitzsch, F., & Potzel, W. 2005, Nuclear Physics B - Proceedings Supplements, 138, 108 , proceedings of the Eighth International Workshop on Topics in Astroparticle and Undeground Physics
Oda, T., Hino, M., Muto, K., Takahara, M., & Sato, K. 1994, Atomic Data and Nuclear Data Tables, 56, 231
Odrzywolek, A. 2005-2010, PSNS code, http://th-www.if.uj.edu.pl/psns/
Odrzywołek, A. 2007, European Physical Journal C, 52, 425
Odrzywolek, A. 2007, Silicon burning neutrinos, http://sn1987a-20th.physics.uci.edu/1630-Odrzywolek.pdf
Odrzywolek, A. 2009, Phys. Rev. C, 80, 045801
Pakmor, R., Kromer, M., Röpke, F. K., et al. 2010, Nature, 463, 61
Phillips, M. M. 2005, in Astronomical Society of the Pacific Conference Series, Vol. 342, 1604-2004: Supernovae as Cosmological Lighthouses, ed. M. Turatto, S. Benetti, L. Zampieri, & W. Shea, 211
Piro, A. L. 2008, ApJ, 679, 616
Piro, A. L. & Bildsten, L. 2008, ApJ, 673, 1009
Plewa, T. 2007, ApJ, 657, 942
Podsiadlowski, P. 2010, Astronomische Nachrichten, 331, 218
Podsiadlowski, P., Mazzali, P., Lesaffre, P., Han, Z., & Förster, F. 2008, New Astronomy Review, 52, 381
Pons, J. A., Steiner, A. W., Prakash, M., & Lattimer, J. M. 2001, Phys. Rev. Lett., 86, 5223
Raghavan, R. S. 1986, Phys. Rev. D, 34, 2088
Raskin, C., Scannapieco, E., Rhoads, J., & Della Valle, M. 2009, ApJ, 707, 74
Riess, A. G., Filippenko, A. V., Challis, P., et al. 1998, AJ, 116, 1009
Riess, A. G., Macri, L., Casertano, S., et al. 2009, ApJ, 699, 539
Rubbia, A. 2009, Journal of Physics: Conference Series, 171, 012020
Ruiter, A. J., Belczynski, K., & Fryer, C. 2009, ApJ, 699, 2026
Ruiz-Lapuente, P., Comeron, F., Méndez, J., et al. 2004, Nature, 431, 1069
Saio, H. & Nomoto, K. 1985, A&A, 150, L21
Sandage, A. & Tammann, G. A. 1993, ApJ, 415, 1
Scannapieco, E. & Bildsten, L. 2005, ApJ, 629, L85
Schawinski, K. 2009, MNRAS, 397, 717
Schinder, P. J., Schramm, D. N., Wiita, P. J., Margolis, S. H., & Tubbs, D. L. 1987, ApJ, 313, 531
Scholberg, K. 2010, Journal of Physics: Conference Series, 203, 012079
Seitenzahl, I. R., Townsley, D. M., Peng, F., & Truran, J. W. 2009, Atomic Data and Nuclear Data Tables, 95, 96
Smartt, S. J. 2009, ARA&A, 47, 63
Smirnov, A. 2009, Workshop Towards Neutrino Technologies, http://cdsagenda5.ictp.trieste.it/full_display.php?ida=a08170
Suzuki, Y. 2001, ArXiv High Energy Physics - Experiment e-prints
Suzuki, Y. 2008, Journal of Physics: Conference Series, 136, 022057
Thielemann, F.-K. 1984, Advances in Space Research, 4, 67
Timmes, F. X., Brown, E. F., & Truran, J. W. 2003, ApJ, 590, L83
Totani, T. & Sato, K. 1995, Astroparticle Physics, 3, 367
Van Der Velde, J. C. et al. 1988, Nucl. Instrum. Meth., A264, 28
Wang, B., Li, X., & Han, Z. 2010, MNRAS, 401, 2729
Webbink, R. F. 1984, ApJ, 277, 355
Whelan, J. & Iben, Jr., I. 1973, ApJ, 186, 1007
Wood-Vasey, W. M., Miknaitis, G., Stubbs, C. W., et al. 2007, ApJ, 666, 694
Woosley, S. E. & Weaver, T. A. 1994, in Supernovae, ed. S. A. Bludman, R. Mochkovitch, & J. Zinn-Justin, 63, given at Les Houches Summer School, Session 54: Supernovae, Les Houches, France, 31 Jul - 1 Sep 1990
Yakovlev, D. G., Kaminker, A. D., Gnedin, O. Y., & Haensel, P. 2001, Physics Reports, 354, 1
Yoon, S. & Langer, N. 2003, A&A, 412, L53
Yoon, S., Podsiadlowski, P., & Rosswog, S. 2007, MNRAS, 380, 933
Zingale, M., Almgren, A. S., Bell, J. B., Nonaka, A., & Woosley, S. E. 2009, ApJ, 704, 196

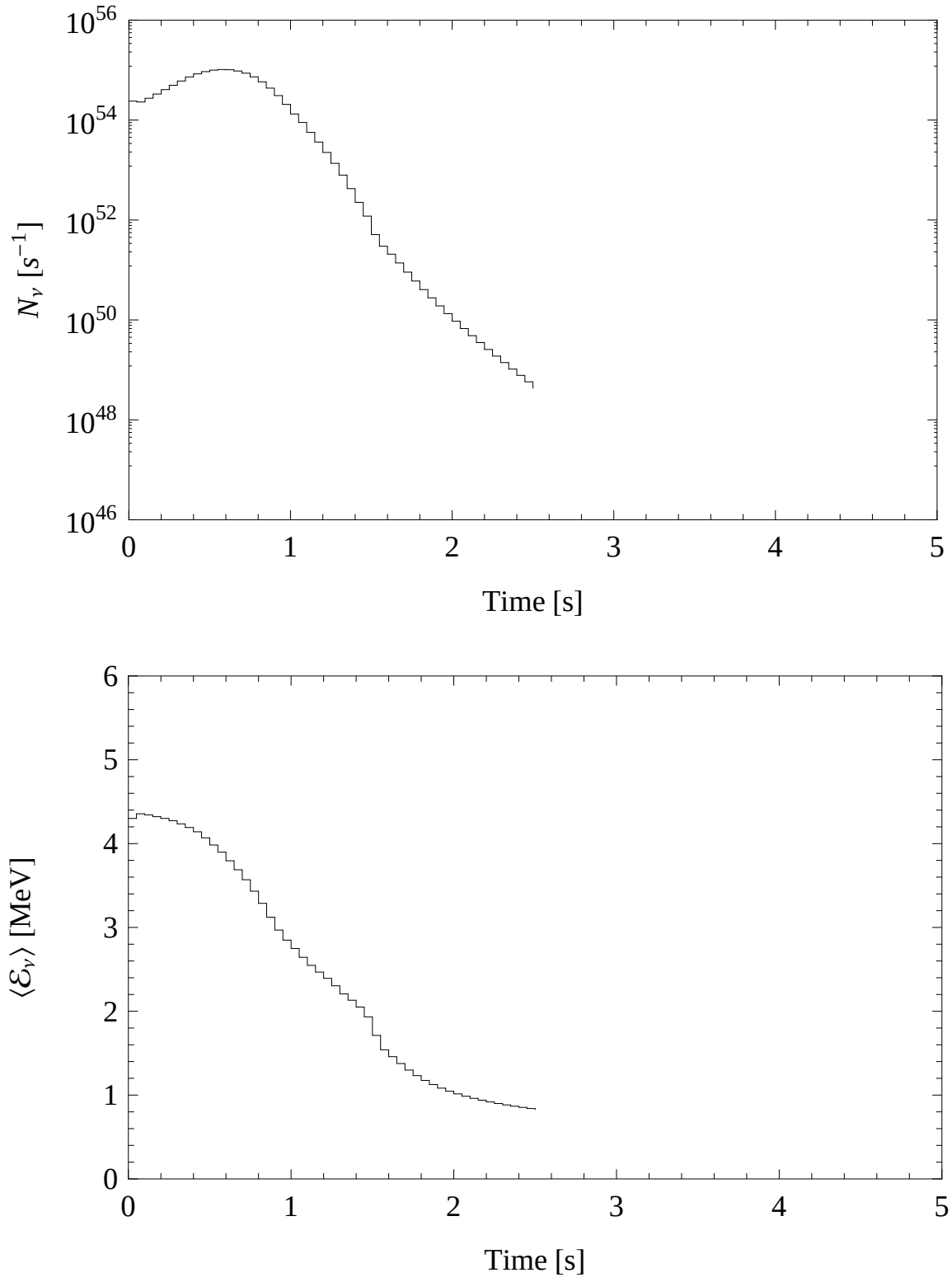

Fig. 9. Model neutrino (ν_e) particle emission in the deflagration model n7d1r10t15c (top). Average neutrino energy (bottom).

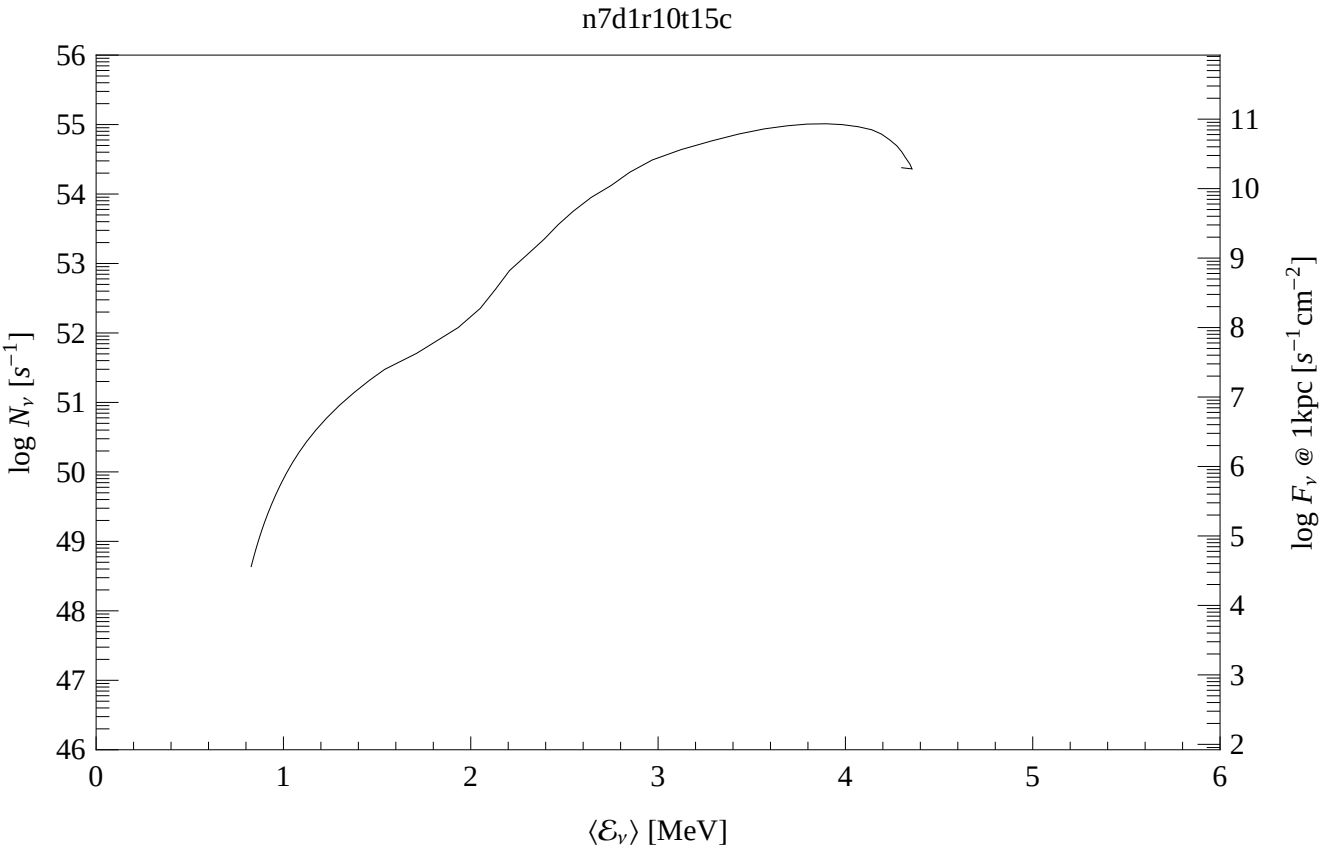

Fig. 10. Total ν_e-HR diagram for the deflagration model n7d1r10t15c.

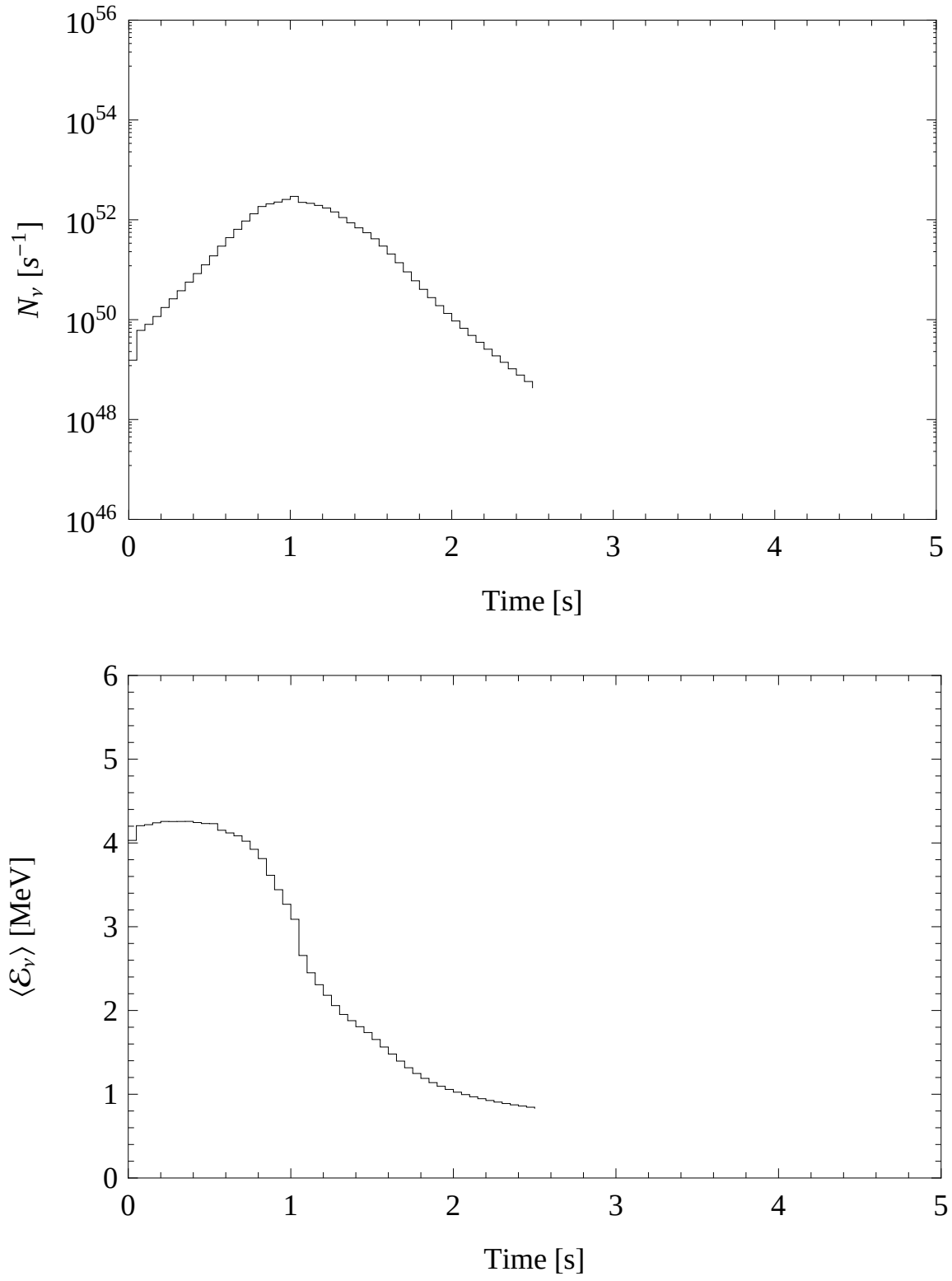

Fig. 11. Model antineutrino ($\bar{\nu}_e$) particle emission in the deflagration model n7d1r10t15c (top). Average antineutrino energy (bottom).

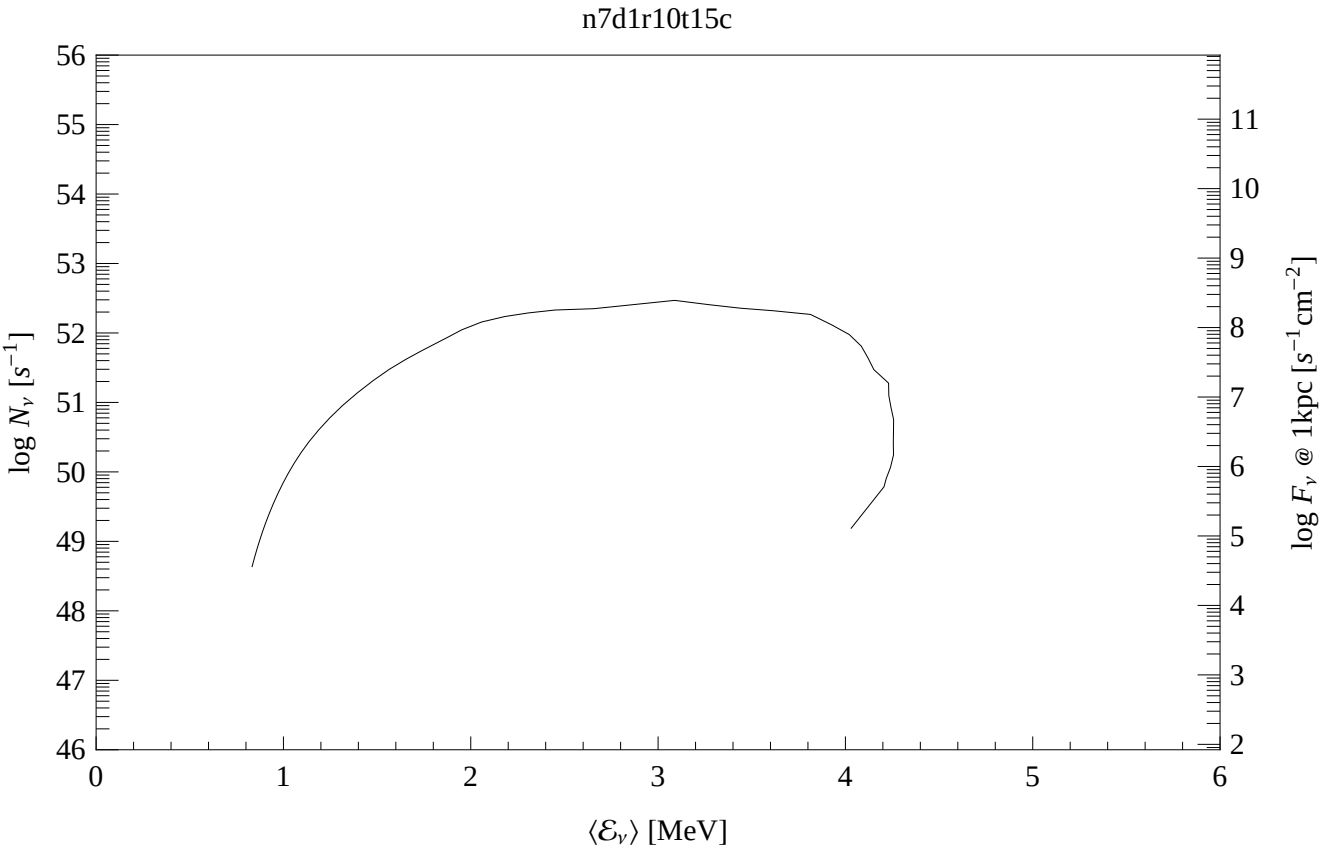

Fig. 12. Total $\bar{\nu}_e$-HR diagram for the deflagration model n7d1r10t15c.

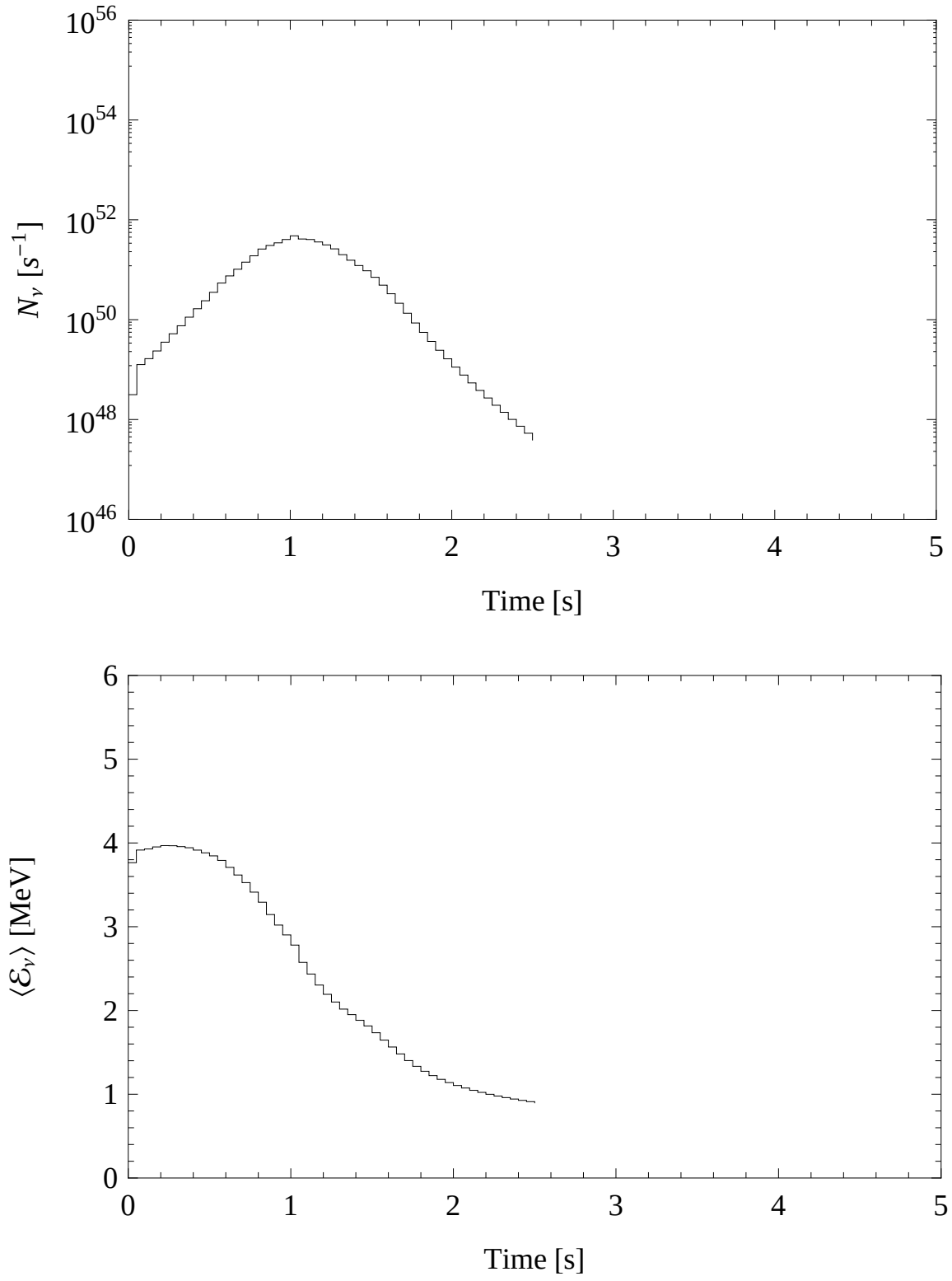

Fig. 13. Model muon/tau neutrino (ν_μ) particle emission in the deflagration model n7d1r10t15c (top). Average neutrino energy (bottom).

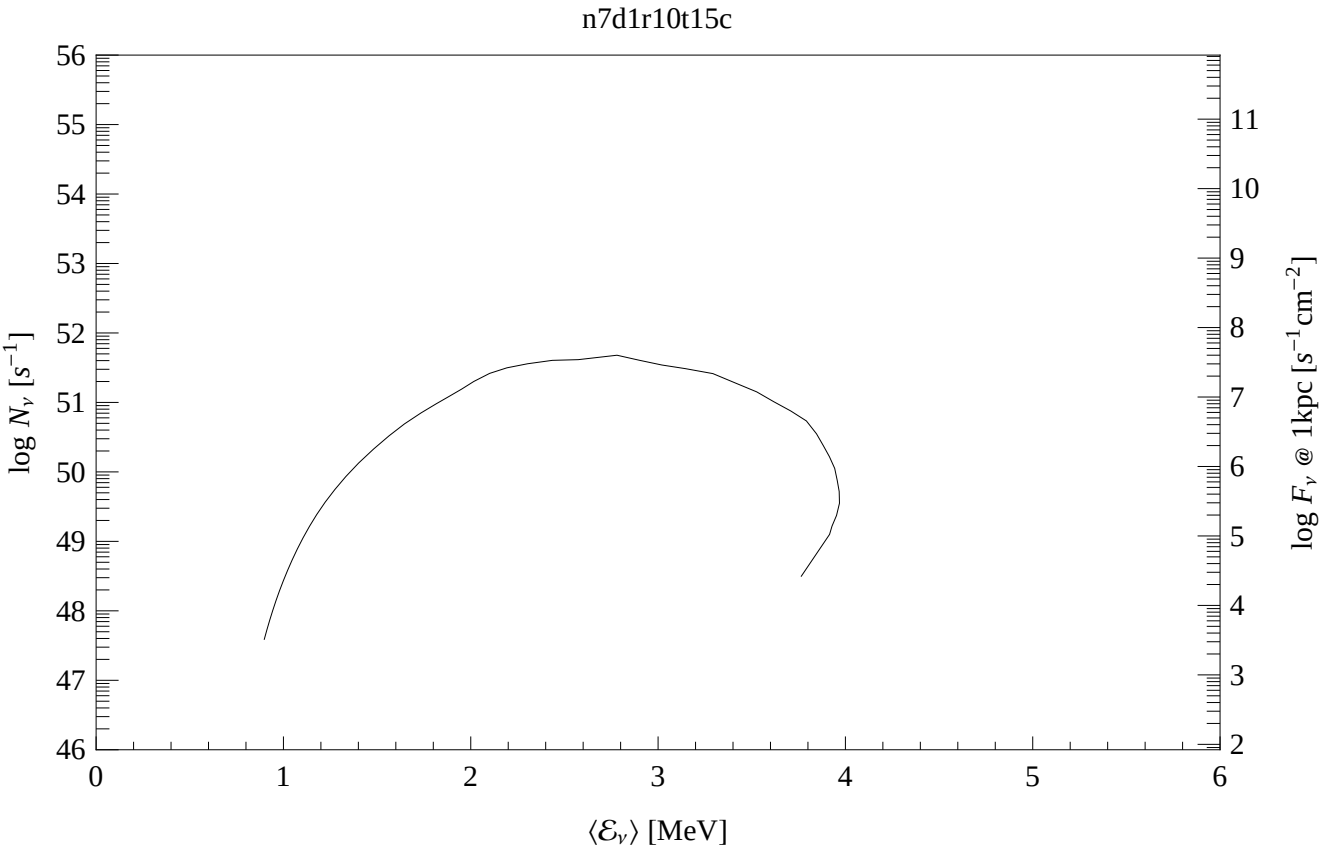

Fig. 14. Total ν_μ-HR diagram for the deflagration model n7d1r10t15c.

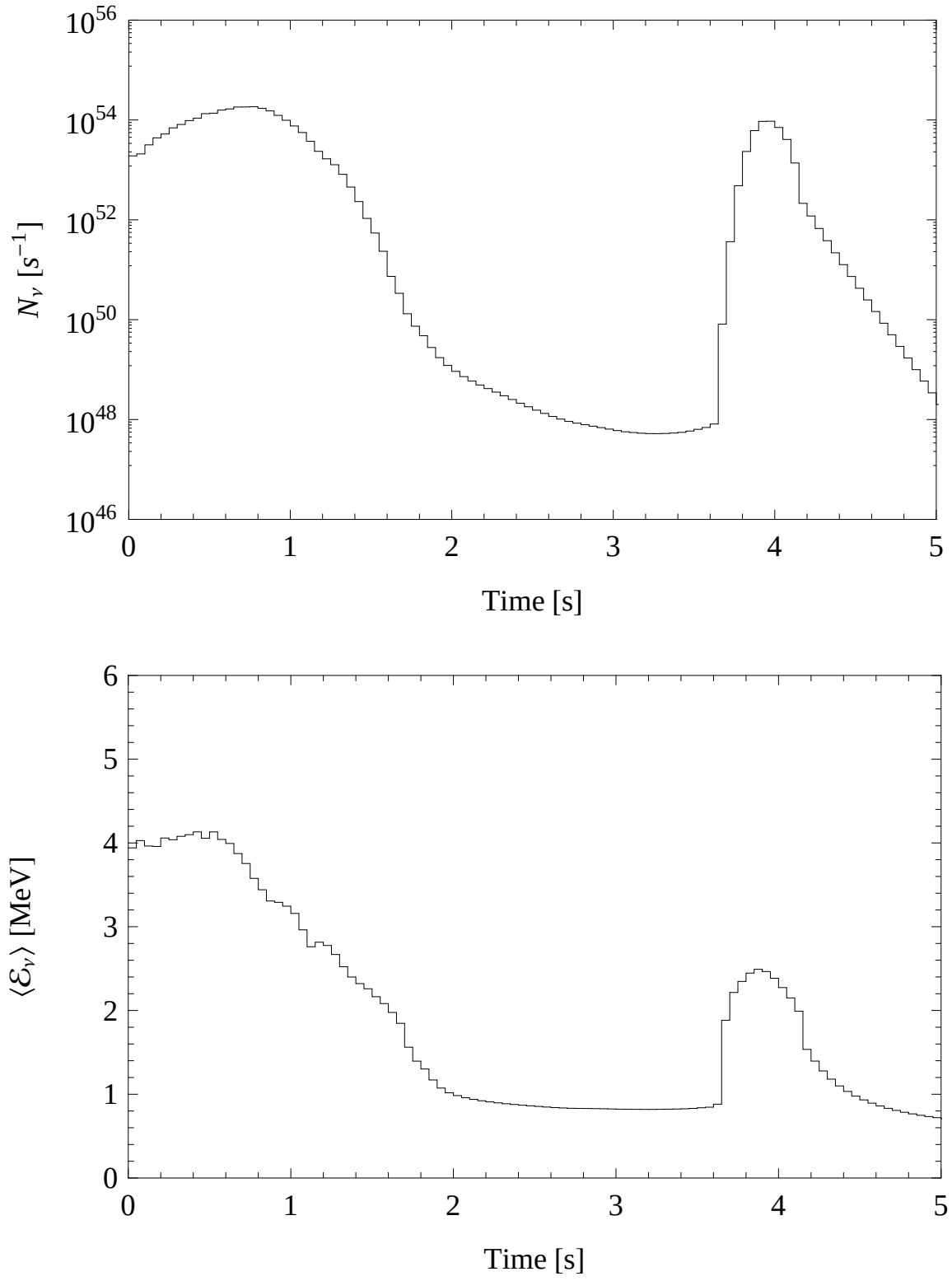

Fig. 15. Model neutrino (ν_e) particle emission in the delayed detonation model Y12 (top). Average neutrino energy (bottom).

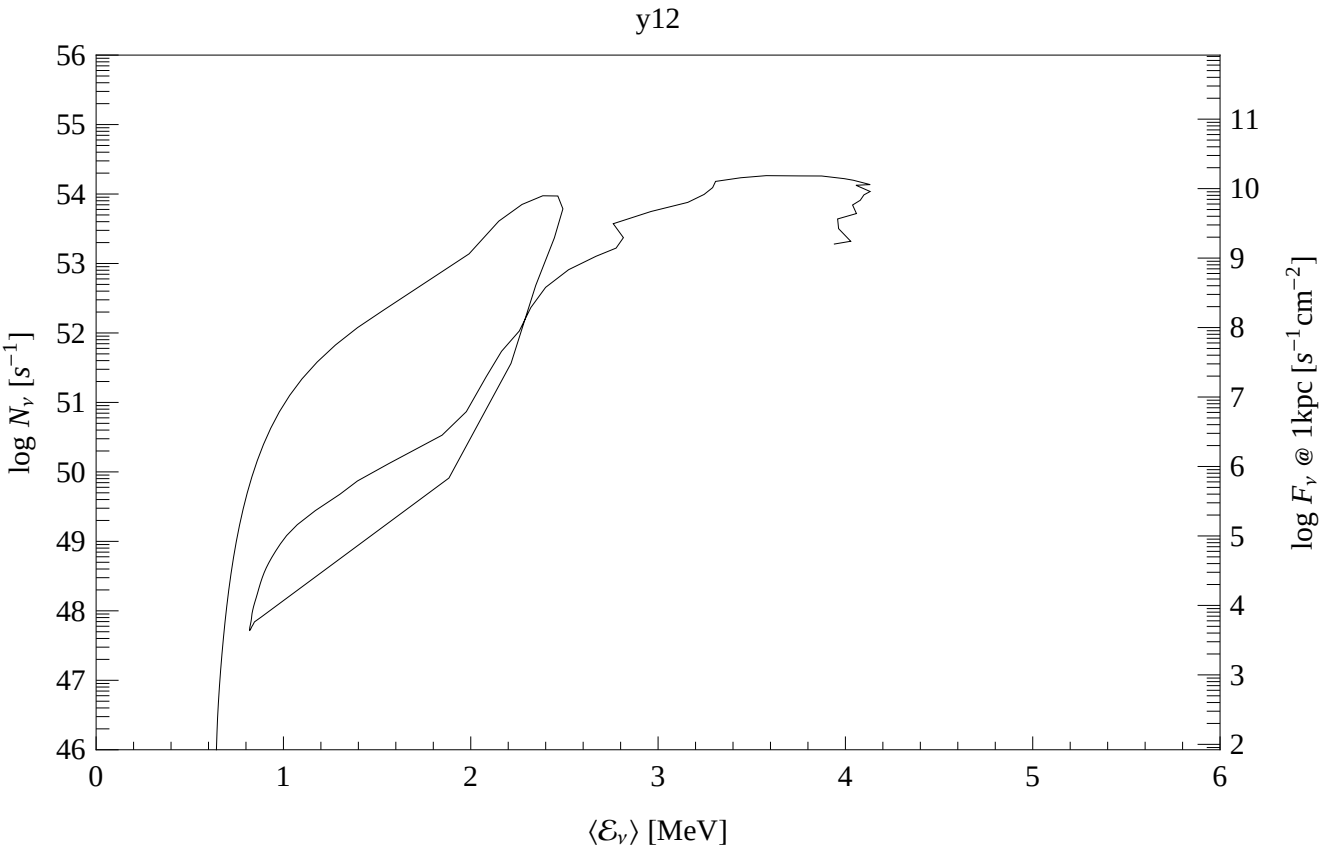

Fig. 16. Total ν_e-HR diagram for the delayed detonation model Y12.

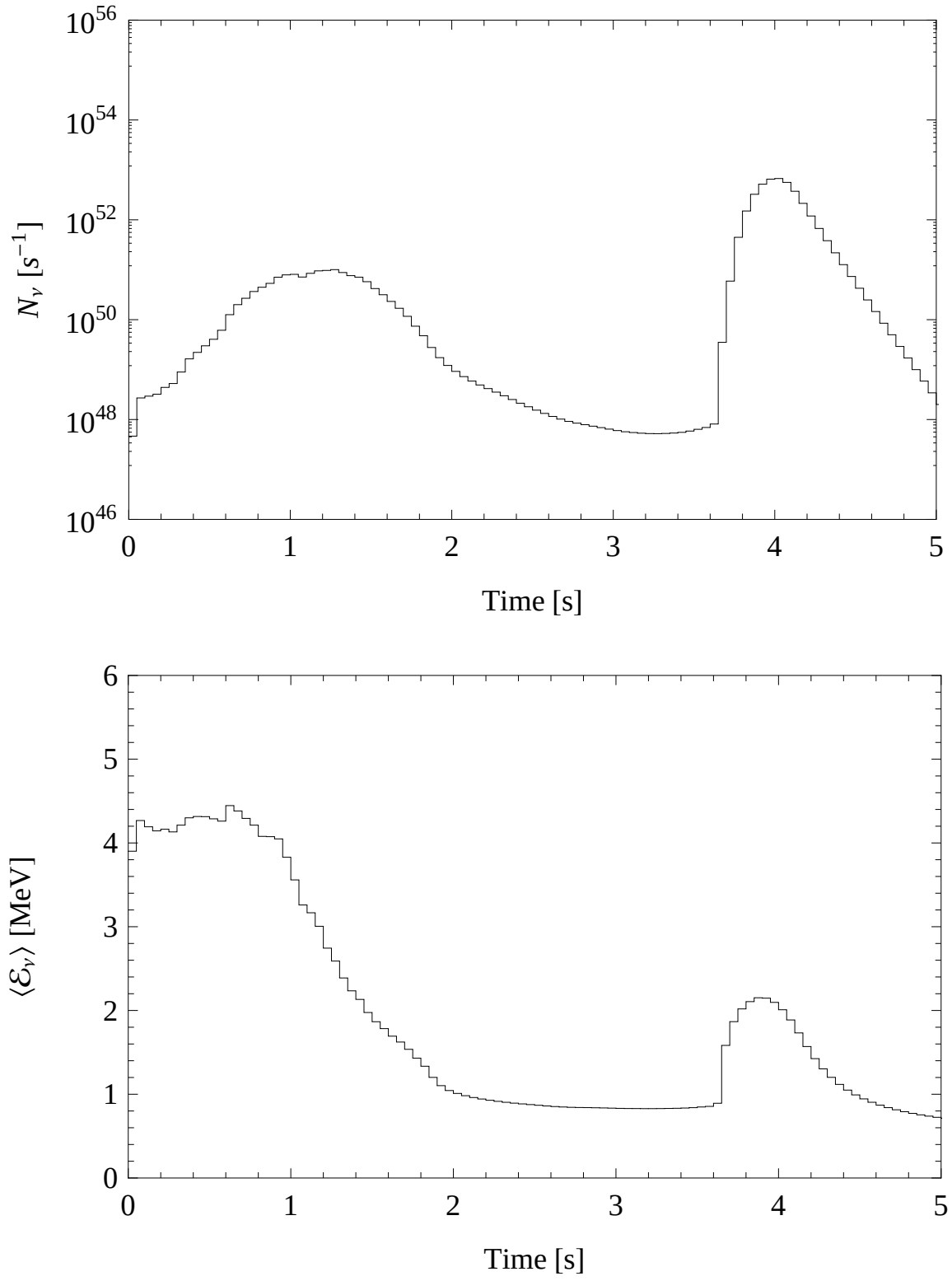

Fig. 17. Model antineutrino ($\bar{\nu}_e$) particle emission in the delayed detonation model Y12 (top). Average antineutrino energy (bottom).

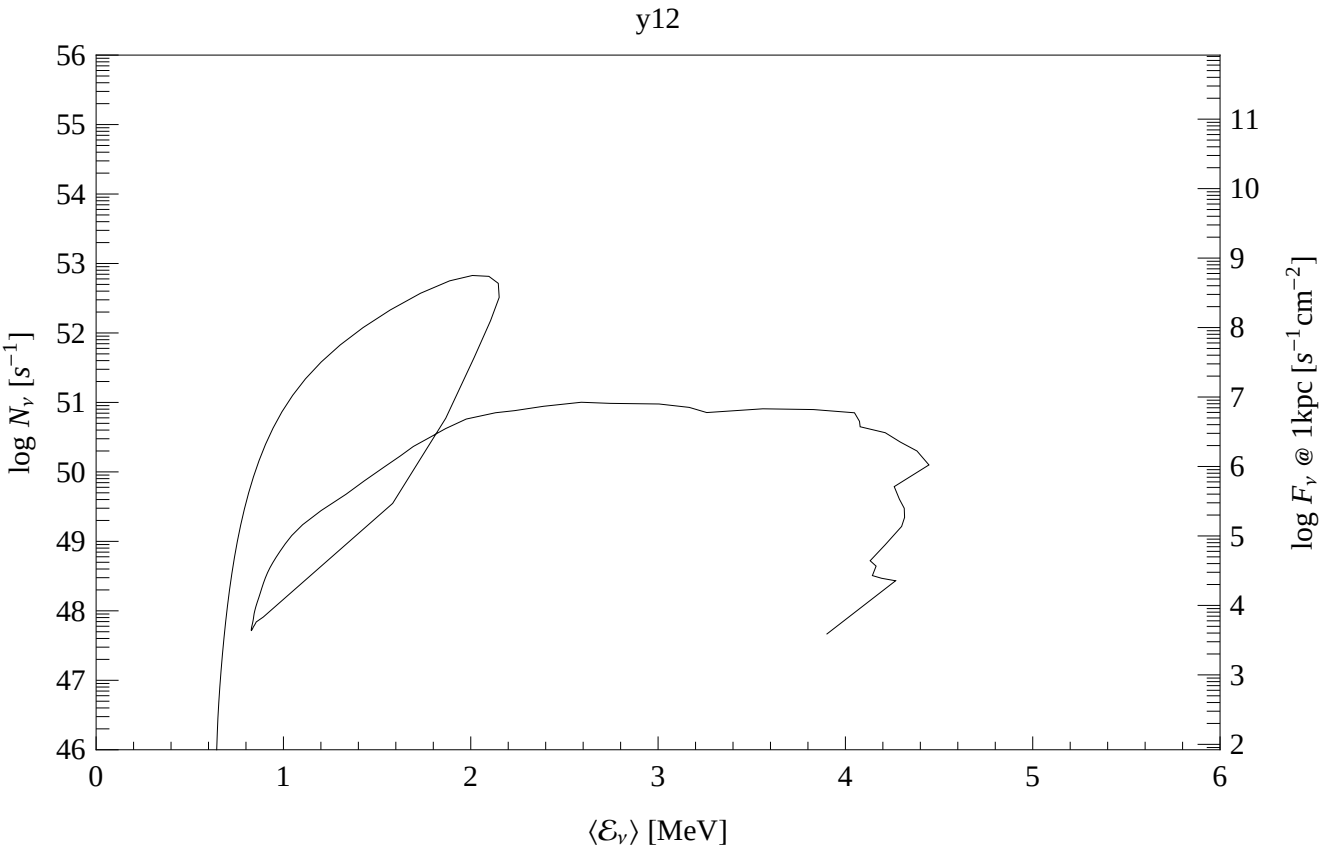

Fig. 18. Total $\bar{\nu}_e$-HR diagram for the delayed detonation model Y12.

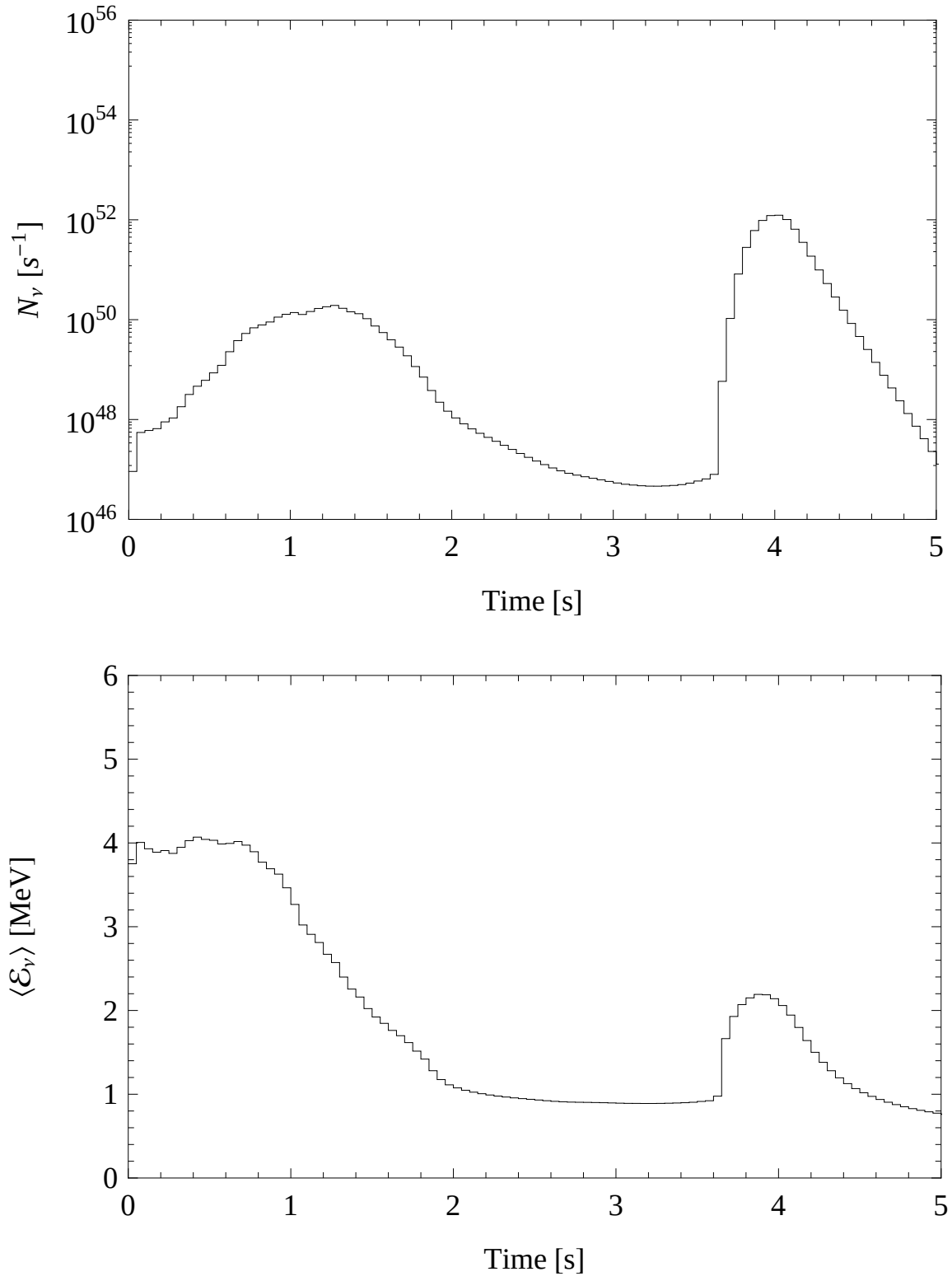

Fig. 19. Model muon/tau neutrino (ν_μ) particle emission in the delayed detonation model Y12 (top). Average neutrino energy (bottom).

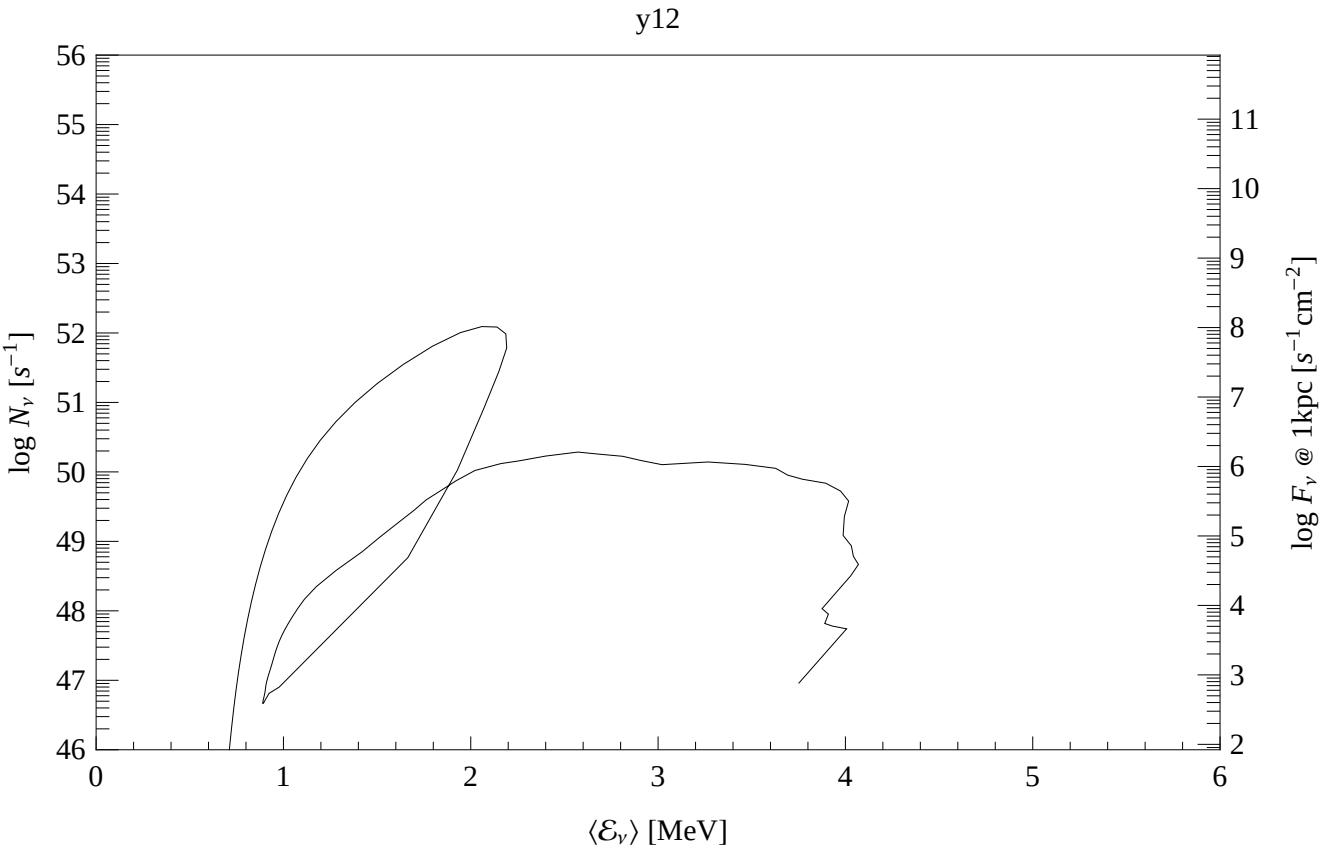

Fig. 20. Total ν_μ-HR diagram for the delayed detonation model Y12.